Uncertainty propagation in dynamic sub-structuring by model reduction integrated domain decomposition

Tanmoy Chatterjee*, Sondipon Adhikari, Michael I. Friswell
College of Engineering, Swansea University, Bay Campus, SA1 8EN, United Kingdom

Abstract

This paper addresses computational aspects in dynamic sub-structuring of built-up structures with uncertainty. Component mode synthesis (CMS), which is a model reduction technique, has been integrated within the framework of domain decomposition (DD), so that reduced models of individual sub-systems can be solved with smaller computational cost compared to solving the full (unreduced) system by DD. This is particularly relevant for structural dynamics applications where the overall system physics can be captured by a relatively low number of modes. The theoretical framework of the proposed methodology has been extended for application in stochastic dynamic systems. To limit the number of eigen-value analyses to be performed corresponding to the random realizations of input parameters, a locally refined high dimensional model representation model with stepwise least squares regression is presented. Effectively, a bi-level decomposition is proposed, one in the physical space and the other in the stochastic space. The geometric decomposition in the physical space by the proposed model reduction-based DD reduces the computational cost of a single analysis of the system and the functional decomposition in the stochastic space by the proposed meta-model lowers the number of simulations to be performed on the actual system. The results achieved by solving a finite-element model of an assembled beam structure and a 3D space frame illustrate good performance of the proposed methodology, highlighting its potential for complex problems.

Keywords: domain decomposition; model reduction; component mode synthesis; Schur complement; functional decomposition; stochastic space

* *Corresponding author* Email: tanmoy.chatterjee@swansea.ac.uk (Tanmoy Chatterjee), s.adhikari@swansea.ac.uk (Sondipon Adhikari), m.i.friswell@swansea.ac.uk (Michael I. Friswell)

1. Introduction

Complex industrial structures generally comprise several components and may be represented by an assembly of relatively simple sub-systems. Analysing full models of such built-up structures can prove to be computationally expensive, even with advanced computational resources. Component mode synthesis (CMS), which is a dynamic sub-structuring and model reduction technique, has proven to be useful in dealing with these assembled systems (Boo et al. 2018). In general, they operate by modelling the sub-components individually and their reduced dynamic models are assembled to form a global system. The literature related to CMS methods is well developed and they have been utilized to solve structural dynamic problems over the past few decades. Extensive reviews of CMS methods can be found in (Craig 2000; Craig and Kurdila 2006; De Klerk et al. 2008).

On the other hand, fast numerical solution techniques involving spatial decomposition in the geometric space, such as domain decomposition (DD) solvers, are relatively newer (as compared to CMS methods) and recently have started to be utilized in industrial applications (Badia et al. 2019a, b; Franceschini et al. 2019). The spatial decomposition is attained through a Schur-complement-based domain decomposition and partitioning. The DD solvers exhibit scalable parallel performance, allowing a significant improvement of model resolution with reduction in computational effort. These methods have mainly been used to solve problems of wave propagation (Sarkar et al. 2009), flow through porous media (Subber and Sarkar 2014) and non-linear oscillators (Subber and Sarkar 2018).

The above approaches (model reduction and DD) adopt different strategies. However, both of them are employed to serve a common purpose, which is to accelerate the solution process of finite element (FE) approximation of partial differential equations (PDEs). In this

regard, the relevant conceptual similarities and differences of these classes of methods have been discussed by (Rixen 2006).

The dynamic response of a structural system is generally predicted by the FE method, in which a deterministic model with a particular set of physical parameters is modelled. However, the underlying assumption is that the set of input parameters to the FE solver is precisely known, and this is not necessarily valid (Mace et al. 2005). The primary reason is the presence of uncertainties in the parameters through the product's entire design cycle and operating service life. Moreover, manufacturing processes can easily lead to variability in the resulting product. Thus, in addition to improve the accuracy of a deterministic model, quantification of the variation in the response due to uncertainty in the input parameters is equally important, if not more so. Previous works on CMS and DD techniques accounting for uncertainties are discussed in the subsequent sections.

However, uncertainty quantification of dynamical systems can be computationally expensive. For direct computation of the frequency response functions (FRF) by inverting the dynamic stiffness matrix as a function of mass, stiffness and damping matrices is expensive as evaluations have to be performed for every value of forcing frequency (Pryse et al. 2018; Lu et al. 2019). Even with multi-output meta-models, such model construction may entail enormous computational resource and CPU/GPU time. Therefore, employing a meta-model which is as accurate as possible over the entire frequency domain while minimizing the computational cost needs to be addressed. A general solution to this problem is employing design of experiments to select a limited set of discrete frequency sample points on which the metamodel is trained, and then utilized to interpolate the response at other frequencies (DiazDelaO et al. 2013). However, the frequency response is characterized by rapid changes at the location of natural frequencies. Such sharp changes make it difficult to select appropriate infill points, which can easily lead to inaccurate representation of resonant peaks and valleys

of the FRF. Another simplified solution commonly used is to predict the representative quantities such as the maximum peaks and resonance frequency positions (Xia and Tang 2013; Wan et al. 2014). However, potentially important information in the FRFs may not be preserved with these simplified approaches.

Therefore, the major challenge associated in dealing with the FRFs as outputs of metamodels is still the high dimensionality. To obtain a more compact description of the functional outputs, multiple feature extraction or data compression techniques have been exploited. With the help of principal component analysis (PCA), the high dimensionality issue was mitigated when the output was expressed as an image of radius over time and angle in (Higdon et al. 2008). Wavelet decomposition was utilized for highly irregular functional time domain data in (Bayarri et al. 2007). A Gibbs sampling-based expectation maximization algorithm was developed to transform the irregularly spaced data into a regular grid so that a Kriging model could be fitted to the functional data in (Hung et al. 2015). The dimension of frequency response data was reduced by using PCA and then the model was updated using a neural network (Sadr et al. 2007). In order to accelerate the convergence of the first two statistical moments of the frequency response in the vicinity of resonance peaks, Aitken's method and its generalization were employed in conjunction with polynomial chaos expansion (PCE) in (Jacquelin et al. 2015). A frequency transformation strategy with a PCA technique was proposed to overcome the limitations of PCE for FRF simulation in (Yaghoubi et al. 2017). Modal analysis was performed to investigate the stochastic dynamic properties of FRFs in (Van den Nieuwenhof, B Coyette 2003; Pichler et al. 2009). PCE models were built for modal properties to predict the bounds for stochastic FRFs in (Manan and Cooper 2010). Aspects, such as dealing with relatively large parameter variations and coping up with the associated variation in modal responses, were addressed using a refined high dimensional model representation (Chatterjee et al. 2016) and multi-output Gaussian process models (Lu et al.

2019). For details, readers are referred to an extensive review of meta-models for stochastic computations (Chatterjee et al. 2019).

Following the above discussion on model-order reduction, domain decomposition and uncertainty quantification in dynamical systems, the primary issues addressed in this work are:

- The existing DD solvers perform computations on the full (unreduced) FE models. This may prove to be computationally expensive for large-scale systems. An improved strategy has been presented in Section 3.
- The above issue may further escalate in presence of uncertainties, where repeated simulations need to be performed. Therefore, a meta-modelling technique has been devised in modal space to propagate the input uncertainty to the frequency response in an efficient manner. This is illustrated in Section 4.2.

The rest of the paper has been organized in the following sequence. Section 2 discusses the basic concepts of the CMS method required for the subsequent contents of the paper. Section 3 presents the proposed deterministic model-order reduced DD method. The stochastic version of the proposed deterministic method is illustrated in Section 4. A numerical study has been carried out in Section 5. Section 6 deals with a large-scale practical structural application. Finally, the key aspects and contribution of the present work have been summarized in Section 7.

2. Component Mode Synthesis

CMS was introduced as early as the 1960s by (Hurty 1965) and (Bampton and Craig 1968). However, the Hurty/Craig-Bampton method is still one of the popular CMS techniques in industry and academia. In CMS, the models of individual sub-structures are transformed from physical space to component modal space with the help of pre-selected basis functions. The

possible choices of these basis functions include normal modes determined from solving a component eigen-value problem and static constraints (Rixen 2004). The models are then assembled and the global response of the whole system is evaluated. Additionally, in applications involving line and surface coupling, the number of interface DOFs can be reduced. A recent comprehensive review regarding the interface reduction can be found in (Krattiger et al. 2019). Next, a brief illustration of the fixed-interface Craig-Bampton method on a two-component structure, as illustrated in Fig. 1, is presented.

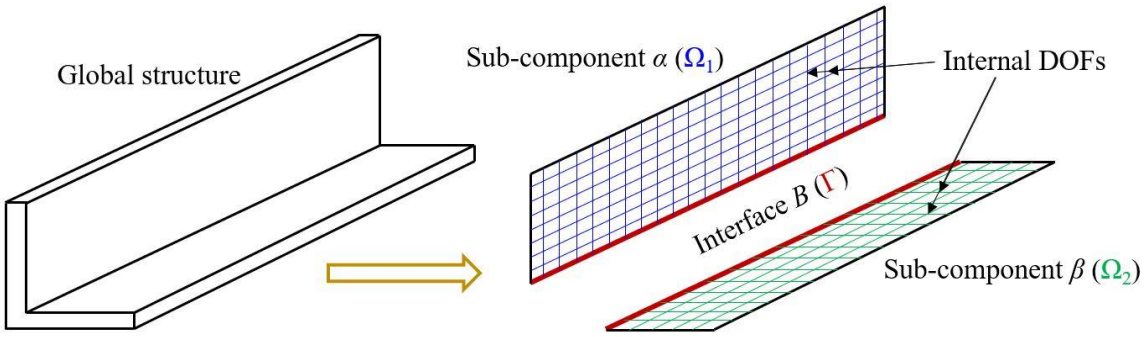

Fig. 1. Illustration of dynamic sub-structuring with the help of an L-section composed of two sub-components.

The equation of motion of component α, without considering the effect of damping, is

$$\mathbf{m}^{\alpha}\ddot{\mathbf{u}}^{\alpha} + \mathbf{k}^{\alpha}\mathbf{u}^{\alpha} = \mathbf{f}^{\alpha} \tag{1}$$

where $\mathbf{m}^{\alpha}, \mathbf{k}^{\alpha}, \mathbf{f}^{\alpha}$ and $\mathbf{u}^{\alpha}$ are the mass and stiffness matrices of component α, the force vector and the physical DOFs, respectively. In the following the α subscript is dropped for clarity. The physical DOFs, $\mathbf{u}$, can be expressed as a set of internal DOFs, $\mathbf{u}_I$, and a set of interface DOFs, $\mathbf{u}_B$, as,

$$\begin{bmatrix}\mathbf{m}_{II} & \mathbf{m}_{IB}\\ \mathbf{m}_{BI} & \mathbf{m}_{BB}\end{bmatrix}\begin{bmatrix}\ddot{\mathbf{u}}_I\\ \ddot{\mathbf{u}}_B\end{bmatrix} + \begin{bmatrix}\mathbf{k}_{II} & \mathbf{k}_{IB}\\ \mathbf{k}_{BI} & \mathbf{k}_{BB}\end{bmatrix}\begin{bmatrix}\mathbf{u}_I\\ \mathbf{u}_B\end{bmatrix} = \begin{bmatrix}\mathbf{f}_I\\ \mathbf{f}_B\end{bmatrix} \tag{2}$$

The fixed-interface normal modes of a component are the eigen-vectors of the component with the interface DOFs fixed. The corresponding eigen-value problem is then

$$\left(\mathbf{k}_{II} - \lambda_j \mathbf{m}_{II}\right)\boldsymbol{\phi}_{I,j} = \mathbf{0}\,, \qquad j = 1, \ldots, n_I \tag{3}$$

Note that the size of the eigen-value problem in Eq. (3) is same as the cardinality of the internal DOFs n_I. The eigenvectors $\boldsymbol{\phi}_{I,j}$ form the columns of the fixed-interface modal matrix. Here, only a subset of the first p modes are retained, and thereby the dimension of the component model is reduced.

In the fixed-interface CMS method, the component modal space consists of the retained fixed-interface normal modes and the static constraint modes, and they are combined to yield the component transformation matrix $\mathbf{G}$ as,

$$\mathbf{G} = \begin{bmatrix} \boldsymbol{\phi}_{Ip} & -\mathbf{k}_{II}^{-1}\mathbf{k}_{IB} \\ \mathbf{0} & \mathbf{I}_{BB} \end{bmatrix} \tag{4}$$

The static constraint modes ensure compatibility of displacements of the components at their interface, enhance convergence and yield the exact static solution. The transformation from physical coordinates, **u,** to component modal coordinates, **q,** is then,

$$\mathbf{u} = \begin{bmatrix} \mathbf{u}_I \\ \mathbf{u}_B \end{bmatrix} = \mathbf{G}\mathbf{q} = \begin{bmatrix} \boldsymbol{\phi}_{Ip} & -\mathbf{k}_{II}^{-1}\mathbf{k}_{IB} \\ \mathbf{0} & \mathbf{I}_{BB} \end{bmatrix} \begin{bmatrix} \mathbf{q}_p \\ \mathbf{q}_c \end{bmatrix} \tag{5}$$

The internal physical coordinates $\mathbf{u}_I$ are transformed into the fixed-interface modal coordinates $\mathbf{q}_p$. The physical interface coordinates $\mathbf{u}_B$ are retained, but are denoted as constraint coordinates $\mathbf{q}_c$. The component modal mass and stiffness matrices $\boldsymbol{\eta} = \mathbf{G^T m G}, \boldsymbol{\nu} = \mathbf{G^T k G}$ take the form,

$$\boldsymbol{\eta} = \begin{bmatrix} \mathbf{I}_{pp} & \mathbf{m}_{pc} \\ \mathbf{m}_{pc}^T & \mathbf{m}_{cc} \end{bmatrix}, \boldsymbol{\nu} = \begin{bmatrix} \boldsymbol{\Gamma}_{pp} & 0 \\ 0 & \mathbf{k}_{cc} \end{bmatrix} \tag{6}$$

where the matrices $\mathbf{m}_{cc}$ and $\mathbf{k}_{cc}$ are the constraint mass and stiffness matrices for component α, $\mathbf{m}_{pc}$ represents a coupled matrix term and $\boldsymbol{\Gamma}_{pp}$ is a diagonal matrix of retained fixed-interface modal eigen-values.

Thus, the equation of motion for component α can be expressed by,

$$\boldsymbol{\eta}^{\alpha}\ddot{\mathbf{q}}^{\alpha} + \boldsymbol{\nu}^{\alpha}\mathbf{q}^{\alpha} = \mathbf{f}_{q}^{\alpha}, \qquad \mathbf{f}_{q}^{\alpha} = \mathbf{G}^{\alpha^{T}}\mathbf{f}^{\alpha} \tag{7}$$

Next, the assembly of two components (say, α and β) is considered. The continuity of displacements at their interface implies $\mathbf{u}_{B}^{\alpha} = \mathbf{u}_{B}^{\beta}$ in the physical space, and is converted into component modal space, such that $\mathbf{q}_{c}^{\alpha} = \mathbf{q}_{c}^{\beta}$. In order to impose the coupling conditions, the following transformation may be applied,

$$\mathbf{q} = \begin{bmatrix} \mathbf{q}_{p}^{\alpha} \\ \mathbf{q}_{c}^{\alpha} \\ \mathbf{q}_{p}^{\beta} \\ \mathbf{q}_{c}^{\beta} \end{bmatrix} = \begin{bmatrix} \mathbf{I} & \mathbf{0} & \mathbf{0} \\ \mathbf{0} & \mathbf{0} & \mathbf{I} \\ \mathbf{0} & \mathbf{I} & \mathbf{0} \\ \mathbf{0} & \mathbf{0} & \mathbf{I} \end{bmatrix} \begin{bmatrix} \mathbf{q}_{p}^{\alpha} \\ \mathbf{q}_{p}^{\beta} \\ \mathbf{q}_{c} \end{bmatrix} \tag{8}$$

After assembling the component modal matrices, the global mass and stiffness matrices take the form,

$$\mathbf{M} = \begin{bmatrix} \mathbf{I}_{pp}^{\alpha} & \mathbf{0} & \mathbf{m}_{pc}^{\alpha} \\ \mathbf{0} & \mathbf{I}_{pp}^{\beta} & \mathbf{m}_{pc}^{\beta} \\ \mathbf{m}_{pc}^{\alpha\,\mathrm{T}} & \mathbf{m}_{pc}^{\beta\,\mathrm{T}} & \mathbf{M}_{cc} \end{bmatrix} \quad \mathbf{K} = \begin{bmatrix} \boldsymbol{\Gamma}_{pp}^{\alpha} & \mathbf{0} & \mathbf{0} \\ \mathbf{0} & \boldsymbol{\Gamma}_{pp}^{\beta} & \mathbf{0} \\ \mathbf{0} & \mathbf{0} & \mathbf{K}_{cc} \end{bmatrix} \tag{9}$$

$$\mathbf{M}_{cc} = \mathbf{m}_{cc}^{\alpha} + \mathbf{m}_{cc}^{\beta}, \qquad \mathbf{K}_{cc} = \mathbf{k}_{cc}^{\alpha} + \mathbf{k}_{cc}^{\beta}$$

Note that the dimension of the global matrices are reduced depending on the number of fixed-interface modes retained in the component modal matrices $\mathbf{G}^{\alpha}$ and $\mathbf{G}^{\beta}$. In this study, we have employed the fixed-interface Craig-Bampton method and therefore interface reduction is not discussed (Krattiger et al. 2019).

After a brief introduction of model-reduction, the proposed methodology in a deterministic sense is illustrated in the next section.

3. Proposed deterministic methodology

3.1 Integrating model-reduction in the framework of domain decomposition

As the name itself suggests, domain decomposition solvers partition the original problem into various sub-problems. In doing so, each of the sub-problems can be computed in parallel using different processors. Several domain decomposition solvers are available depending on whether the sub-domains are overlapping or non-overlapping (Bjorstad et al. 1996). Here, we employ the generalized framework of DD for non-overlapping sub-domains as proposed by (Sarkar et al. 2009) to illustrate the improvements.

Considering the whole domain Ω of the FE model of an arbitrary system in an *n*-dimensional subspace partitioned into two non-overlapping sub-domains Ω_1 and Ω_2, as shown in Fig. 1, the dynamic equation of motion of the system in the frequency domain is,

$$\begin{bmatrix} [\mathbf{D}_{II}^{\alpha}]_{n_1\times n_1} & \mathbf{0} & [\mathbf{D}_{IB}^{\alpha}]_{n_1\times n_B} \\ \mathbf{0} & \left[\mathbf{D}_{II}^{\beta}\right]_{n_2\times n_2} & \left[\mathbf{D}_{IB}^{\beta}\right]_{n_2\times n_B} \\ [\mathbf{D}_{BI}^{\alpha}]_{n_B\times n_1} & \left[\mathbf{D}_{BI}^{\beta}\right]_{n_B\times n_2} & \left[\mathbf{D}_{BB}^{\alpha}+\mathbf{D}_{BB}^{\beta}\right]_{n_B\times n_B} \end{bmatrix} \begin{Bmatrix} \mathbf{x}_I^{\alpha} \\ \mathbf{x}_I^{\beta} \\ \mathbf{x}_B \end{Bmatrix} = \begin{Bmatrix} \mathbf{f}_I^{\alpha} \\ \mathbf{f}_I^{\beta} \\ \mathbf{f}_B^{\alpha}+\mathbf{f}_B^{\beta} \end{Bmatrix} \tag{10}$$

where $\mathbf{D}_{ij}^{s} = (-\omega^2\mathbf{M}_{ij}^{s} + i\omega\mathbf{C}_{ij}^{s} + \mathbf{K}_{ij}^{s})$ denotes the dynamic stiffness matrix. The superscript *s* represent the sub-system α or β and the subscripts $ij = II, BB$ and IB refer to the internal DOFs, interface DOFs and coupling DOFs, respectively (following the same notation as Section 2).

It is often observed that for engineering dynamics applications, mesh refinement is required to capture complex geometries, leading to a high number of modes. This results in a significant increase in the size of the resulting system (represented by Eq. (10)) from the FE model. However, in most structural applications, it is found that the dynamics can be captured by a relatively low number of linear modes (Hinke et al. 2009). Taking advantage of this useful feature, we have integrated model-reduction (specifically CMS) into the framework of domain

decomposition so as to avoid solving the full system in Eq. (10) and efficiently evaluate the dynamic response. This will be quite straightforward to follow as the Craig-Bampton method has already been discussed in the previous section.

Carrying out the operations in Eqs. (4)-(6) on individual sub-systems α and β, leads to a reduced assembled system obtained as,

$$\begin{bmatrix} \left[\mathbf{D}_{II}^{\alpha'}\right]_{n_1' \times n_1'} & \mathbf{0} & \left[\mathbf{D}_{IB}^{\alpha'}\right]_{n_1' \times n_B} \\ \mathbf{0} & \left[\mathbf{D}_{II}^{\beta'}\right]_{n_2' \times n_2'} & \left[\mathbf{D}_{IB}^{\beta'}\right]_{n_2' \times n_B} \\ \left[\mathbf{D}_{BI}^{\alpha'}\right]_{n_B \times n_1'} & \left[\mathbf{D}_{BI}^{\beta'}\right]_{n_B \times n_2'} & \left[\mathbf{D}_{BB}^{\alpha} + \mathbf{D}_{BB}^{\beta}\right]_{n_B \times n_B} \end{bmatrix} \begin{Bmatrix} \mathbf{x}_I^{\alpha'} \\ \mathbf{x}_I^{\beta'} \\ \mathbf{x}_B \end{Bmatrix} = \begin{Bmatrix} \mathbf{f}_I^{\alpha'} \\ \mathbf{f}_I^{\beta'} \\ \mathbf{f}_B^{\alpha} + \mathbf{f}_B^{\beta} \end{Bmatrix} \tag{11}$$

Remark 1. Note that the internal DOFs of individual sub-systems α and β are reduced from n_1 and n_2 in Eq. (10) to n_1' and n_2', respectively, in Eq. (11), based on the number of fixed-interface modes retained in the component modal matrices $\mathbf{G}^{\alpha}$ and $\mathbf{G}^{\beta}$ (Eq. (4)). n_1 and n_2 denote the number of unreduced internal DOFs of sub-systems α and β, respectively. Whereas n_1' and n_2' represent the number of retained internal DOFs of sub-systems α and β, respectively after model reduction.

3.2 Efficient solution scheme by Schur complement

The reduced system of equations represented by Eq. (11) can be partitioned and rearranged in the following form,

$$\left(\underbrace{\left[\mathbf{D}_{BB}^{\alpha}\right]-\left[\mathbf{D}_{BI}^{\alpha'}\right]\left[\mathbf{D}_{II}^{\alpha'}\right]^{-1}\left[\mathbf{D}_{IB}^{\alpha'}\right]}_{\mathbf{S}_1}+\underbrace{\left[\mathbf{D}_{BB}^{\beta}\right]-\left[\mathbf{D}_{BI}^{\beta'}\right]\left[\mathbf{D}_{II}^{\beta'}\right]^{-1}\left[\mathbf{D}_{IB}^{\beta'}\right]}_{\mathbf{S}_2}\right)\{\mathbf{x}_B\}$$
$$=\left[\underbrace{\left\{\mathbf{f}_B^{\alpha}\right\}-\left[\mathbf{D}_{BI}^{\alpha'}\right]\left[\mathbf{D}_{II}^{\alpha'}\right]^{-1}\left\{\mathbf{f}_I^{\alpha'}\right\}}_{\mathbf{F}_1}\right]+\left[\underbrace{\left\{\mathbf{f}_B^{\beta}\right\}-\left[\mathbf{D}_{BI}^{\beta'}\right]\left[\mathbf{D}_{II}^{\beta'}\right]^{-1}\left\{\mathbf{f}_I^{\beta'}\right\}}_{\mathbf{F}_2}\right] \tag{12}$$

$$\left[\mathbf{D}_{II}^{\alpha'}\right]\left\{\mathbf{x}_I^{\alpha'}\right\}=\mathbf{f}_I^{\alpha'}-\left[\mathbf{D}_{IB}^{\alpha'}\right]\{\mathbf{x}_B\} \tag{13}$$

$$\left[\mathbf{D}_{II}^{\beta'}\right]\left\{\mathbf{x}_I^{\beta'}\right\}=\mathbf{f}_I^{\beta'}-\left[\mathbf{D}_{IB}^{\beta'}\right]\{\mathbf{x}_B\} \tag{14}$$

The interface DOFs can be solved using Eq. (12). The coefficient matrix $\mathbf{S}=\mathbf{S}_1+\mathbf{S}_2$ is referred to as the Schur complement matrix. The size of $\mathbf{S}$ is smaller than the coefficient matrix in Eq. (11) and furthermore $\mathbf{S}_1$ and $\mathbf{S}_2$ can be constructed in parallel. Once the interface problem is solved, $\mathbf{x}_B$ can be substituted into Eqs. (13) and (14) to obtain the response at the internal DOFs $\mathbf{x}_I^{\alpha'}$ and $\mathbf{x}_I^{\beta'}$. It is also worth mentioning that the solutions for $\mathbf{x}_I^{\alpha'}$ and $\mathbf{x}_I^{\beta'}$ can be executed in parallel. To solve the interface problem when the order of $\mathbf{x}_B$ is very high, iterative methods such as the conjugate gradient method can be used for computational tractability (Bjorstad et al. 1996).

Remark 2. (i) Since the proposed approach utilizes the reduced model that is solved by the DD method, the terms to be inverted (i.e. dynamic stiffness matrices corresponding to the internal DOFs of sub-systems $\mathbf{D}_{II}^{\alpha'}$ and $\mathbf{D}_{II}^{\beta'}$ to solve Eqs. (12)-(14)) are much lower in dimension compared to the conventional DD performed on the full system. For an explicit quantification of the improvement in the cost involved, the computational complexities of $\left[\mathbf{D}_{II}^{\alpha'}\right]^{-1}$ and $\left[\mathbf{D}_{II}^{\beta'}\right]^{-1}$ are reduced to $O\left({n_1'}^3\right)$ and $O\left({n_2'}^3\right)$ from $O\left({n_1}^3\right)$ and $O\left({n_2}^3\right)$, respectively. (ii) From an implementation and coding perspective, once these inverse terms have been computed in

Eq. (12), they can be stored and readily utilized in Eqs. (13) and (14). (iii) Also, the coupling matrices $\left[\mathbf{D}_{BI}^{\alpha'}\right]$, $\left[\mathbf{D}_{IB}^{\alpha'}\right]$, $\left[\mathbf{D}_{BI}^{\beta'}\right]$ and $\left[\mathbf{D}_{IB}^{\beta'}\right]$ involved in the multiplicative operations in Eq. (12) result in a lower cost due to the reduced components arising from the internal DOF part. For implementation of the inverse operation, the backslash operator (x = A\b) in MATLAB® has been utilized. This operator yields the solution using Gaussian elimination, without forming the inverse explicitly. For further computational enhancement, parallelized preconditioned conjugate gradient solvers for stochastic partial differential equations proposed in (Subber 2012) can be employed. This iterative algorithm eliminates the need of explicit construction of the Schur complement system. Such iterative sub-structuring techniques in conjunction with the reduced Schur complement system employed here is expected to yield further computational leverage.

Remark 3. Although, this work does not actively deal with unreduced matrices, it is worth mentioning that if one is dealing with unreduced systems, sparse direct or iterative solvers can lead to significant advantage both in terms of storage and computational effort as compared to full/dense solvers. For efficient memory usage and minimum floating point operations, the numerical implementation of such algorithms should exploit the multi-level sparsity structure of the coefficient matrix of the stochastic system, namely (i) the sparsity (unstructured) structure due to the finite element discretization and (ii) the block sparsity structure arising from the orthogonal representation and projection of the stochastic processes. For details of efficient algorithmic implementation of sparse solvers, the reader is referred to (Saad 2003; Subber 2012) and '*Sparse Matrix Operations*' help documentation page of MATLAB® toolbox.

3.3 Reduced model-based domain decomposition for multiple sub-domains

In the previous sub-sections, the proposed CMS based DD was presented in case of two sub-domains to give an explicit mathematical formulation. In this section, the formulation will be generalized for the case of multiple sub-domains; although this extension is straightforward theoretical, giving explicit mathematical expressions that cover all possible interfaces between pairs of sub-structures is more difficult.

The global interface response vector $\{\mathbf{x}_B\}$ is defined as the concatenation of the responses at all of the individual interfaces. In the presence of n_{sd} sub-domains, there will be at most $\frac{1}{2}n_{sd}(n_{sd}-1)$ interfaces between pairs of sub-domains, and indeed interface nodes can be part of more than two sub-domains. However, $\{\mathbf{x}_B\}$ contains all DOFs associated with any interface node. Extending Eq. (12), the interface response can be calculated from

$$\sum_{k=1}^{n_{sd}}\left(\left[\mathbf{D}_{BB}^{k}\right]-\left[\mathbf{D}_{BI}^{k'}\right]\left[\mathbf{D}_{II}^{k'}\right]^{-1}\left[\mathbf{D}_{IB}^{k'}\right]\right)\{\mathbf{x}_B\}=\sum_{k=1}^{n_{sd}}\left(\{\mathbf{f}_B^{k}\}-\left[\mathbf{D}_{BI}^{k'}\right]\left[\mathbf{D}_{II}^{k'}\right]^{-1}\{\mathbf{f}_I^{k'}\}\right) \tag{15}$$

where $\mathbf{D}_{ij}^{k}$ is the dynamic stiffness submatrix for the k th sub-domain, where ij = II, IB, BI or BB as before. The superscript k' denotes the reduced model of the k th sub-domain. The external forces $\{\mathbf{f}_B^{k}\}$ and $\{\mathbf{f}_I^{k'}\}$ for the k th sub-domain are defined at the interface and reduced internal DOFs. However, any particular sub-domain will not contain all of the interface DOFs. Hence, for example, $\left[\mathbf{D}_{BB}^{k}\right]$ will contain many zero rows and zero columns, and the non-zeros terms will correspond to those interface DOFs that are present in the k th sub-domain. Subsequently, the response at the reduced internal DOFs of the k th sub-domain are obtained as

$$\left[\mathbf{D}_{II}^{k'}\right]\{\mathbf{x}_I^{k'}\}=\mathbf{f}_I^{k'}-\left[\mathbf{D}_{IB}^{k'}\right]\{\mathbf{x}_B\},\qquad \text{for } k=1,2,\dots,n_{sd} \tag{16}$$

As illustrated previously in the case of two sub-domains, the evaluation of the Schur complement matrix and the resulting forcing vector term on the right side of Eq. (15) and Eq. (16) is parallelizable for each sub-domain. Alternatively, a more compact representation can be found in (Sarkar et al. 2009) where a restriction matrix consisting of zeros and ones for each sub-domains (Bjorstad et al. 1996) is used to establish a link between the global interface variable and local interface variables.

In the next section, the implementation of the proposed approach in stochastic systems is illustrated.

4. Proposed stochastic methodology

This section has been divided into two sub-sections. The first sub-section briefly reviews the recent and significant works on CMS and DD specifically applied to stochastic systems. Although unconventional at this stage of the paper, this is expected to benefit readers to track the state-of-the-art of the multi-disciplinary theme. The second sub-section illustrates the functional decomposition in the stochastic space and efficient implementation of the proposed methodology in presence of parametric uncertainties.

4.1 Recent works on CMS and DD only applied to stochastic systems

CMS combined with perturbation methods for quantifying the uncertainty in the structural dynamic response have been studied by (Hinke et al. 2009; Sarsri and Azrar 2016). In the presence of a high level of input uncertainty (when the perturbation methods do not generally work well), efficient stochastic reduced basis projection schemes (Nair and Keane 2002) have been utilized with CMS for the modelling and propagation of spatially distributed joint

uncertainties (Dohnal et al. 2009). Polynomial chaos expansion (PCE) in conjunction with CMS has been used to compute the frequency response functions (FRFs) of stochastic systems (Sarsri et al. 2011). (Soize and Chebli 2003) performed non-parametric uncertainty modelling (Soize 2000) in the Craig-Bampton approach using random matrices and the entropy optimization principle. More recently, a variant of the CMS technique based on dominant fixed-interface normal modes and the static contribution of higher order modes has been developed (Jensen et al. 2017). The utility of the study lies in the fact that the residual normal modes are invariant with the modification of structural system parameters and thus can be effectively utilized in re-analysis based problems within limited computational budget. A reduced order modelling technique was proposed for uncertainty propagation in time-invariant problems (González et al. 2019). The construction of the projection basis only consists of a single system analysis and a sensitivity analysis.

For the first time, Sarkar et al. (Sarkar et al. 2009) proposed a theoretical framework for the non-overlapping DD of stochastic systems. This was extended to solve large-scale spectral stochastic FE simulations (Subber and Sarkar 2013, 2014). The intrusive PCE based non-overlapping DD methods with preconditioned conjugate gradient (PCG) techniques have illustrated excellent scalability for problems with high mesh resolution (Subber 2012; Subber and Sarkar 2013, 2014). However, the solvers suffered from large memory requirements and computational issues while handling uncertainty quantification of practical engineering applications involving a fine level of discretization in both spatial and stochastic spaces. Recently, the above critical issues have been alleviated to a considerable extent using scalable sparse iterative solvers with efficient preconditioners to deal with problems involving large numbers of random variables and high mesh resolution at the same time (Desai et al. 2018). An efficient scheme of time integration for strongly non-linear stochastic systems has been

presented (Subber and Sarkar 2018), which has the potential to solve stochastic PDEs in conjunction with spatial DD.

Next, the implementation of the proposed methodology is illustrated in presence of parametric uncertainties.

4.2 Functional decomposition in the stochastic space

Repeated simulations will be required in order to compute the system response corresponding to the random realizations of the input parameters. Monte Carlo simulations (MCS) performed on the proposed model-reduction based DD would require a smaller computational effort compared to DD of the unreduced system. However, we would still like to reduce the computational cost further by limiting the number of actual function evaluations.

The basic idea is to approximate the eigen-vectors of the retained DOFs of the model-reduced sub-structures by using a meta-model and then performing the DD and Schur complement operations based on meta-model predictions of the reduced system. To be specific, the term $\boldsymbol{\phi}_{Ip}$ of the component modal matrix in Eq. (5) is estimated via the meta-model. This will lead to the following advantages: (i) First and foremost, only n_{samp} eigen-value analyses have to be performed, where n_{samp} denote the number of training samples for the meta-model, compared to n_{MCS} eigen-value analyses, where n_{MCS} is the number of MCS samples and $n_{\mathrm{samp}} \ll n_{\mathrm{MCS}}$. (ii) As the response quantity of interest is only the eigen-vectors, which is the outcome of a linear analysis, considerably simpler meta-models can be expected to perform adequately in terms of approximation accuracy. (iii) To some extent, the accuracy aspect of the meta-model may be compromised as a trade-off with computational cost in the case of large-scale systems, as it is well known that the effect of eigen-vectors on the dynamic response is not particularly strong.

Therefore to limit the number of eigen-value analyses, functional decomposition in the stochastic space is performed using locally refined high dimensional model representation (HDMR). In doing so, Kriging (Dubourg 2011) has been combined with HDMR (Li et al. 2006) to capture the local variations in the functional space. This concept was first utilized by (Kersaudy et al. 2015) to enhance the local approximation capabilities of PCE and later on to improve HDMR (Chatterjee et al. 2016; Chatterjee and Chowdhury 2018a). To determine the unknown coefficients and ensure the orthogonality of the component functions, a stepwise least squares (SLS) approach has been adopted here as proposed by (Li et al. 2006). Next, the computational framework of the proposed locally refined HDMR with SLS is presented in a concise manner.

Let, $\boldsymbol{x} = (x_1, x_2, \dots, x_N)$ be the vector of random input parameters defined by their joint probability density function $f_{\mathbf{X}}(\boldsymbol{x})$, where $\boldsymbol{x} \in D \subset \mathbb{R}^N$. The meta-model response $\hat{g}(\boldsymbol{x})$ (here in this case, eigen-vectors) can be expressed as

$$\hat{g}(\boldsymbol{x}) = [g_0 + \underbrace{\sum_i \sum_k \alpha_k^i \psi_k(x_i)}_{\text{first-order}} + \underbrace{\sum_{1 \le i < j \le N} \left(\sum_k \alpha_k^{(ij)i} \psi_k(x_i) + \sum_k \alpha_k^{(ij)j} \psi_k(x_j) + \sum \sum \alpha_{mn}^{(ij)} \psi_m(x_i) \psi_n(x_j) \right)}_{\text{second-order}} + \cdots \text{up to } M^{\text{th}} \text{order}] + \underbrace{\sigma^2 \boldsymbol{Z}(\boldsymbol{x})}_{\text{Kriging}} \quad (17)$$

Eq. (17) represents a Kriging model with the trend portion replaced by second order HDMR. ψ and α represent the basis functions and unknown coefficients, respectively. g_0 is a constant term representing the zeroth order component function or the mean response obtained corresponding to the training samples. $\boldsymbol{Z}(\boldsymbol{x})$ and σ^2 are a zero mean, unit variance Gaussian

process and the process variance, respectively. The HDMR functional form in Eq. (17) consists of independent (first-order) terms within the second order component functions. This is known as extended basis formulation and details regarding it can be found in (Li et al. 2006). It is to be noted that the bases ψ satisfy the following orthogonality relation,

$$\mathbb{E}\left[\psi_{\mathbf{i}}\psi_{\mathbf{j}}\right] = m\delta_{\mathbf{ij}}\,, \qquad 0 \le |\mathbf{i}|, |\mathbf{j}| \le n, \qquad m \ge 0 \tag{18}$$

where,

$$\delta_{\mathbf{ij}} = \prod_{k=1}^{n} \delta_{i_k j_k} = 1, \quad \text{if } \mathbf{i} = \mathbf{j}$$
$$= 0, \quad \text{elsewhere} \tag{19}$$

Where, the notation $\mathbf{i} = (i_1, i_2, \ldots, i_N)$ denotes a multi-index with $|\mathbf{i}| = i_1 + i_2 + \cdots + i_N$. Based on the orthogonality criteria as illustrated in Eq. (18), the appropriate polynomial bases are to be selected. In this context, generalized polynomial chaos from the Askey scheme of hypergeometric orthogonal polynomials (Xiu and Karniadakis 2002) has been utilized in Eq. (17).

From the standard Kriging literature, the unknown coefficients can be determined by solving the following system of equations,

$$(\boldsymbol{\psi}^{\boldsymbol{T}}\boldsymbol{R}^{-\mathbf{1}}\boldsymbol{\psi})\boldsymbol{\alpha}^{*} = \boldsymbol{\psi}^{\boldsymbol{T}}\boldsymbol{R}^{-\mathbf{1}}\boldsymbol{d} \tag{20}$$

where $R_{ij} = \boldsymbol{R}\left(\boldsymbol{x}^{(i)}, \boldsymbol{x}^{(j)}; \boldsymbol{\theta}\right)$ represents the auto-correlation matrix of the points in the experimental design. $\boldsymbol{\theta}$ denotes the hyperparameters and $\boldsymbol{\alpha}^{*}$ is the vector of unknown coefficients. $\boldsymbol{d} = \hat{\boldsymbol{g}}(\boldsymbol{x}) - g_0$ is a vector given by the difference between the observed system response at the training samples $\hat{\boldsymbol{g}}$ and the mean response g_0. The unknown coefficient vector can be determined by direct inversion of the coefficient matrix of Eq. (20). However, in order to ensure the orthogonality of the component functions and the uniqueness of the solution, the

vector of unknown coefficients has been obtained by SLS regression approach proposed in (Li et al. 2006).

In doing so, the coefficients corresponding to the first order component functions are first determined followed by the coefficients of the second order component functions by least square regression and hence the name '*stepwise*' least squares. An important point to note is that this approach is also applicable for dependent random variables, nevertheless in this work, it is illustrated for independent random variables as a special case of the general treatment.

The model form in Eq. (17) by combining Kriging and HDMR in conjunction with the SLS regression approach to determine the unknown coefficients will be referred to as the proposed meta-model (PM) from now onwards.

To help understanding, a flowchart is shown in Fig. 2 to illustrate the proposed model reduction based DD in stochastic systems (Sections 3 and 4). It can be observed from Fig. 2 that the proposed methodology consists of two blocks indicated by the dotted rectangles. This is illustrated to separate the meta-model building part which involves limited number of high-fidelity simulations (computationally expensive as they involve actual FE analysis) and MCS which involves large number of low-fidelity simulations (cheap to compute as it is performed on the meta-model). Once the training input samples are generated and the corresponding response (mode shape vectors of individual sub-components) are evaluated, the meta-model form can be constructed by using Eq. (17). Evaluating Eq. (17) at the training samples yield the systems of equations in Eq. (20), from which the unknown coefficient vector is solved by SLS regression approach. Note that the meta-model is only trained to approximate the mode shape vectors up to the retained modes of individual sub-systems as the reduced configuration is already selected in a deterministic sense corresponding to the nominal values of input parameters.

Subsequently, MCS is performed on the meta-model to obtain the approximate eigen-vectors of the individual sub-systems. Using these estimated eigen-vectors, the component transformation matrix in Eq. (4) is formed, resulting in reduced system matrices of individual sub-systems in Eq. (9). Now the reduced system matrices of the sub-systems are repartitioned and assembled as shown in Eq. (11) and solved efficiently with the help of Eqs. (12)-(14). The frequency response functions of the assembled system are computed for each MCS realization. The uncertainty propagated in the assembled system response due to the random input parameters of the individual sub-systems are quantified by the global FRF statistics.

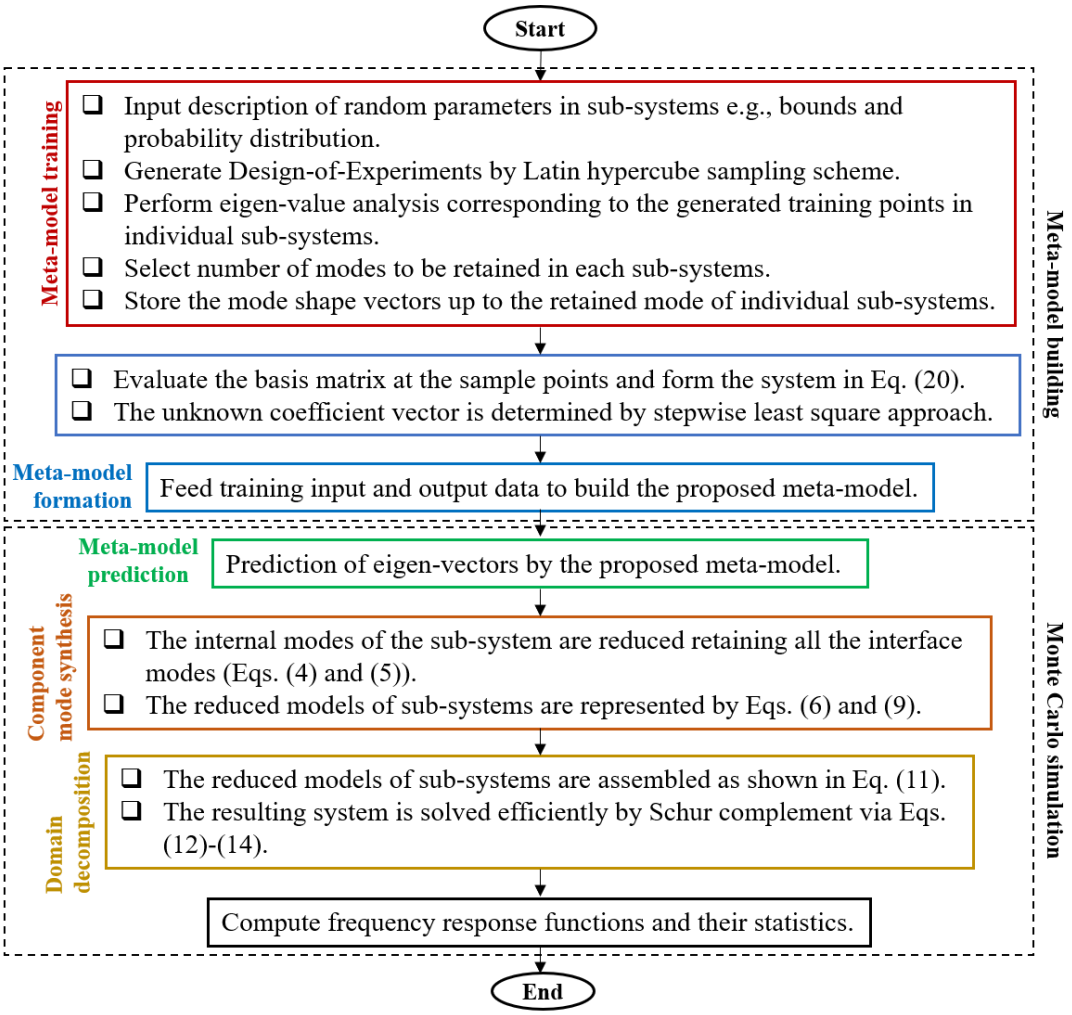

Fig. 2. Flowchart of the proposed methodology.

At this stage, it is reasonable to illustrate the computational efficiency achieved by the proposed methodology. The computational effort required to solve stochastic static/dynamic systems can be expressed as a function of the cost of one analysis and the number of simulations to be performed corresponding to the random input realizations.

$$\begin{aligned}&\text{Computational effort}\\&= f(\text{cost of a single analysis, number of actual simulations})\\&= \text{cost of a single analysis x number of actual simulations}\end{aligned} \tag{21}$$

By using the proposed methodology, the cost of a single analysis can be reduced due to the model reduction performed within the DD framework as illustrated in Section 3, and the number of actual simulations can be reduced by the meta-modelling technique presented in Section 4. Thus, a two-tier improvement of both aspects of computational cost can be achieved by the bi-layered decomposition in the physical and functional space.

To the authors' knowledge, this implementation of the stochastic version of model reduction based DD is first of its kind. Therefore, the main objective has been to present the theoretical framework in a simplistic manner in the context of dynamic sub-structuring. More importantly, the implementation of the proposed methodology is generalized so that recent improvements of CMS and DD can be seamlessly incorporated within the framework. In addition, any available meta-modelling tools can be used for the functional decomposition of the stochastic space.

5. Numerical case study

After illustrating the theoretical framework of the proposed methodology, it is now applied to solve a simple assembled structural problem. The structure consists of FE models of two Euler-Bernoulli cantilever beams connected at their free ends as shown in Fig. 3. Two case studies

of the same example problem have been considered. The first case study involves a symmetric configuration where the two sub-components are equal in length and divided into equal numbers of elements (Fig. 3(a)), whereas the second case (Fig. 3(b)) considers an asymmetric configuration where the sub-components are unequal in length and divided into an unequal number of elements. The asymmetric case is primarily studied as it replicates a more common practical scenario where the sub-components may be of different shape and size. Moreover, the number of modes to be retained for model reduction in the sub-components should be different for the asymmetric case.

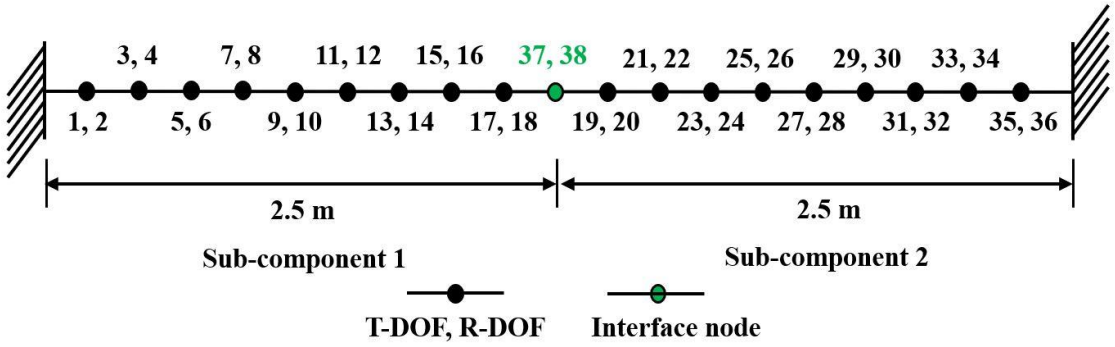

(a)

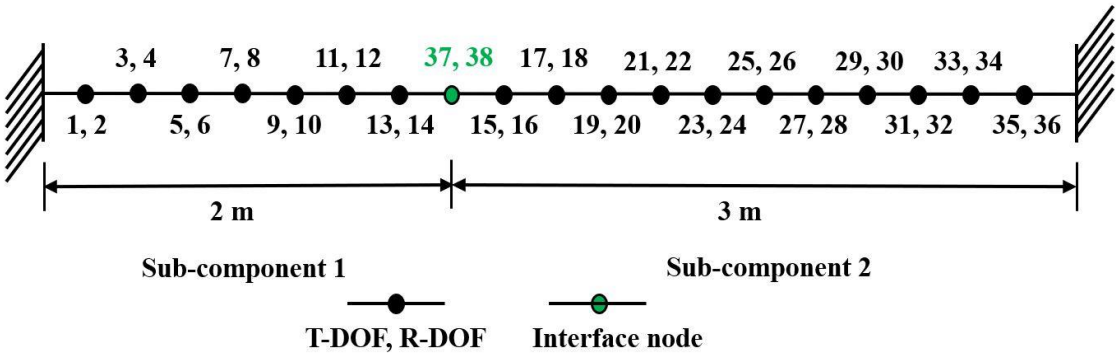

(b)

Fig. 3. Schematic diagram of the FE model of the assembled beam structure (a) Case I: Two components of equal length and (b) Case II: Two components of unequal length. T-DOF and R-DOF denote translational and rotational degree of freedom.

Nominal values of material density, namely $\rho = 2700\ \text{kg/m}^3$, elastic modulus $E =$ 70 GPa and a square cross-sectional dimension with width 0.5 m, are adopted for both cases. The damping of the system is assumed to be of the form $\mathbf{C} = \theta\,\mathbf{K}$, where the parameter θ is

assumed to be 10^{-6}, and **K** is the stiffness matrix. The total length of the assembled structure is 5 m. In case I, each component has ten elements with nine internal nodes and hence eighteen internal DOFs (Fig. 3(a)). Whereas in the second case, component 1 has eight elements, seven internal nodes and fourteen internal DOFs and component 2 has twelve elements, eleven internal nodes and twenty-two internal DOFs (Fig. 3(b)).

Generally, in order to determine the minimal number of modes required, the convergence of the natural frequencies or strain energy is studied and the modes lower than the cut-off frequency are retained and the higher ones are ignored. However, the cut-off frequency entirely depends on the type of dynamic application. Thus, in our case where the motive is to illustrate the framework of the proposed methodology and is not limited to a particular application, we adopt a generalized approach for determining the number of modes to be retained for model reduction of the sub-components via CMS.

The error obtained in the deterministic response by considering varying number of modes was computed. The error was computed in three steps, first the Frobenius norm of the frequency response matrix is determined for every forcing frequency, second, the relative L2 error of the Frobenius norm corresponding to the reduced model with respect to the full model is computed and lastly, the root mean square (RMS) of the relative L2 error has been obtained. Convergence plots of this error obtained with number of retained modes for cases I and II are presented in Figure 4.

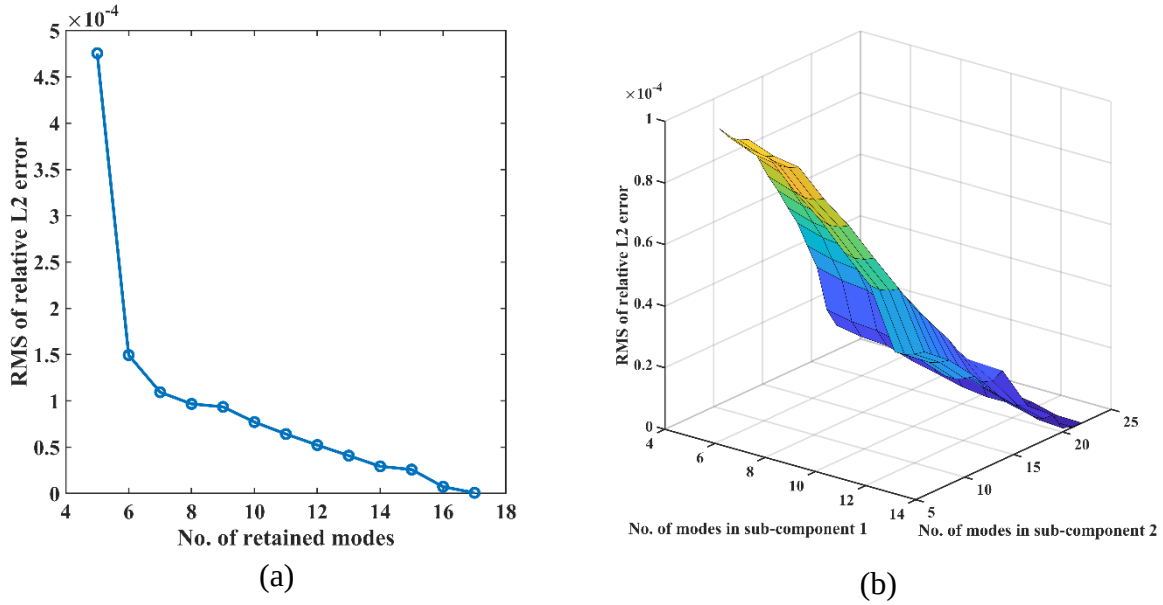

(a) (b)

Figure 4. Convergence of RMS of relative L2 error of the Frobenius norm of the frequency response of the reduced model with respect to the full model with varying number of retained modes (a) Case I (the number of retained internal modes are equal for both sub-components) (b) Case II.

Based on the convergence study presented in Fig. 4, the number of internal DOFs for sub-components 1 and 2 are taken as 6 and 6, respectively for case I and the number of internal DOFs for sub-components 1 and 2 are taken as 5 and 8, respectively for case II without any significant loss of accuracy in capturing the full model based assembled response. This means a 66.7% reduction in computations compared to the full model in each sub-system for case I and 64.3% and 63.6% reduction in computations compared to the full model in sub-system 1 and 2, respectively for case II, can be achieved due to the above configuration of the reduced model.

The forcing frequency range up to 5000 rad/s has been considered (which is almost 800 Hz). To simulate the randomness in the system, the material and geometric properties of each discretized element of the individual sub-systems is considered as stochastic. Specifically, the density, elastic modulus and cross-sectional dimension of each element is considered to be

lognormally distributed with 10% variation. The mean of these parameters is the same as their nominal values reported above.

In this paper, a Gaussian correlation function has been utilized to build the Kriging part (Mukhopadhyay et al. 2016). 35 training points have been generated with a Latin-hypercube sampling scheme (McKay et al. 1979) to construct the proposed meta-model. The PM is trained to approximate the eigen-vectors corresponding to the retained internal DOFs of individual sub-structures.

The first six modes retained out of the eighteen corresponding to each sub-system in case I leads to a mode shape matrix of dimension (18 x 6) and the first five and eight modes retained out of fourteen and twenty-two, respectively in sub-systems 1 and 2 in case II lead to mode shape matrices of dimension of (14 x 5) and (22 x 8). Thus, considering each term of the mode shape matrix, the total number of quantities to be approximated are: Case I: sub-system 1 - (18 x 6 = 108), sub-system 2 – (18 x 6 = 108) and Case II: sub-system 1 - (14 x 5 = 70), sub-system 2 – (22 x 8 = 176). Subsequently, the stochastic frequency responses of the assembled system are obtained by solving the model reduced DD framework as illustrated in Eqs. (12)-(14) in conjunction with the PM based prediction of the mode shapes. In doing so, the effect of component level uncertainty on the assembled system level response is efficiently quantified.

Remark 4. The uncertainty propagation problem in the proposed CMS integrated DD framework is shown in Fig. 5. Note that in the proposed methodology, only the part concerned with uncertainty propagation from the component physical to the component modal level requires few actual simulations. Apart from this, the subsequent levels of uncertainty propagation such as component modal to global modal and then to global physical level are cost effective as the computations involved are primarily based on meta-model predictions.

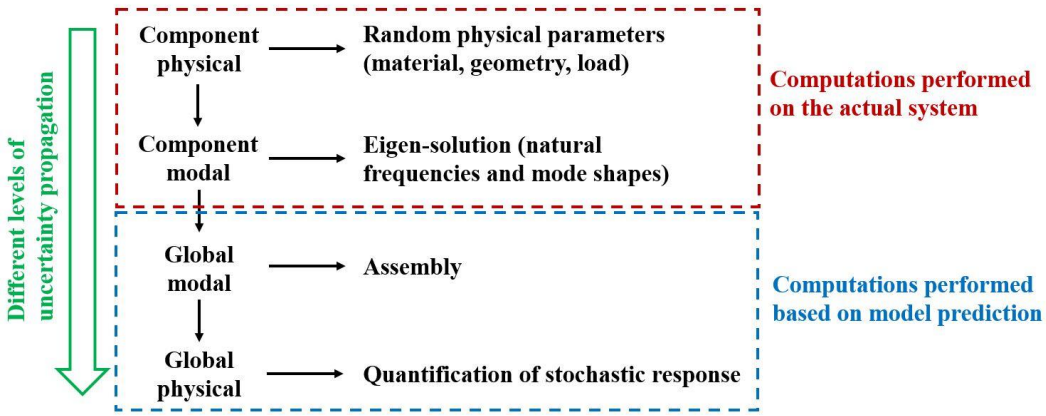

Fig. 5. A schematic representation of different levels of uncertainty propagation in assembled structures.

Sample results have been presented below in Fig. 6 and Fig. 7 in terms of displacement FRF band plots for cases I and II, respectively. Close proximity between the predicted (on the right side) and actual results (on the left side) illustrate good approximation accuracy is obtained.

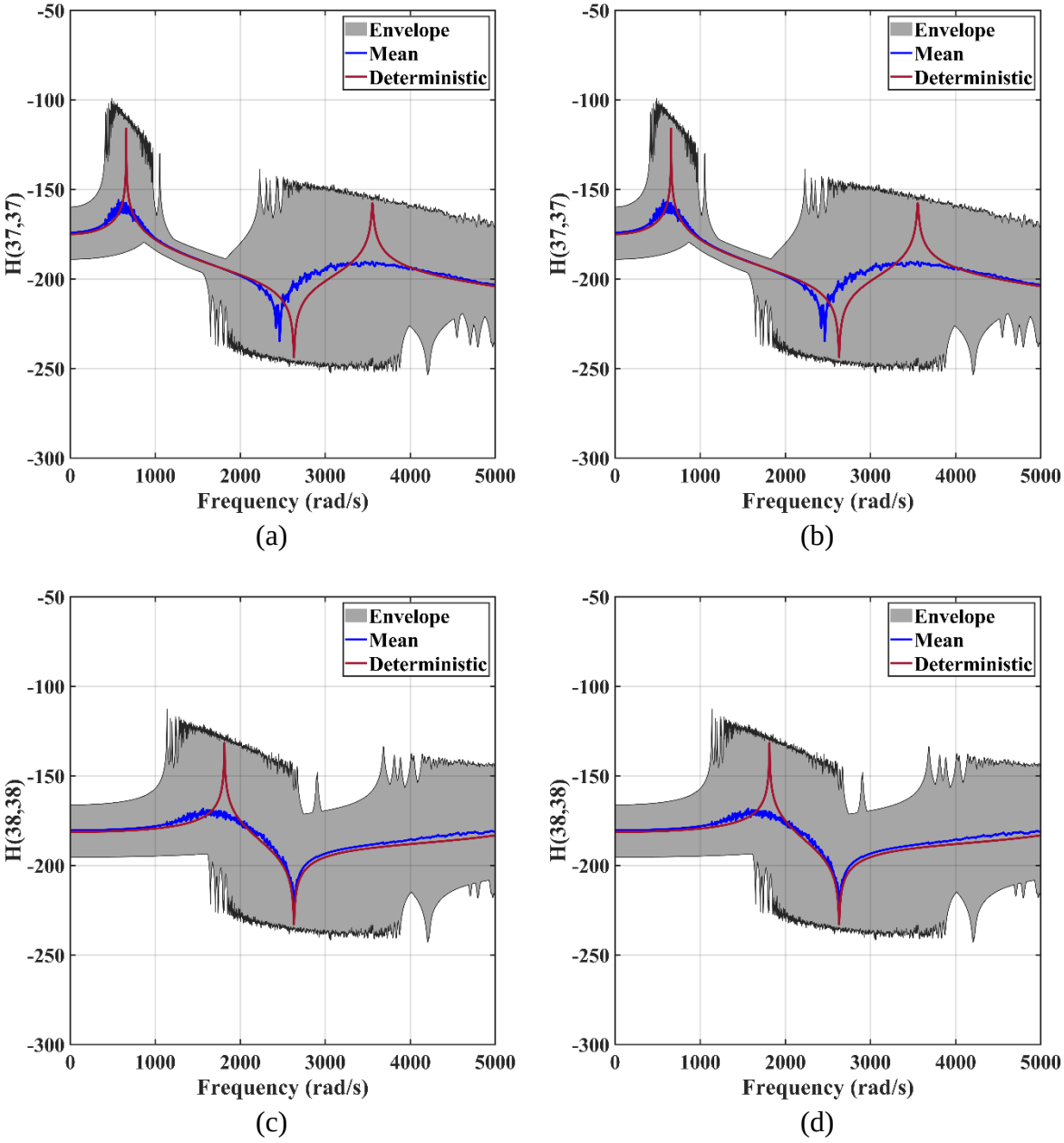

Fig. 6. Displacement FRF band plots (dB) in case I: H(37,37) (a) MCS (b) PM, H(38,38) (c) MCS (d) PM. Note that 10^4 MCS samples are performed. 35 training points have been employed to construct the PM.

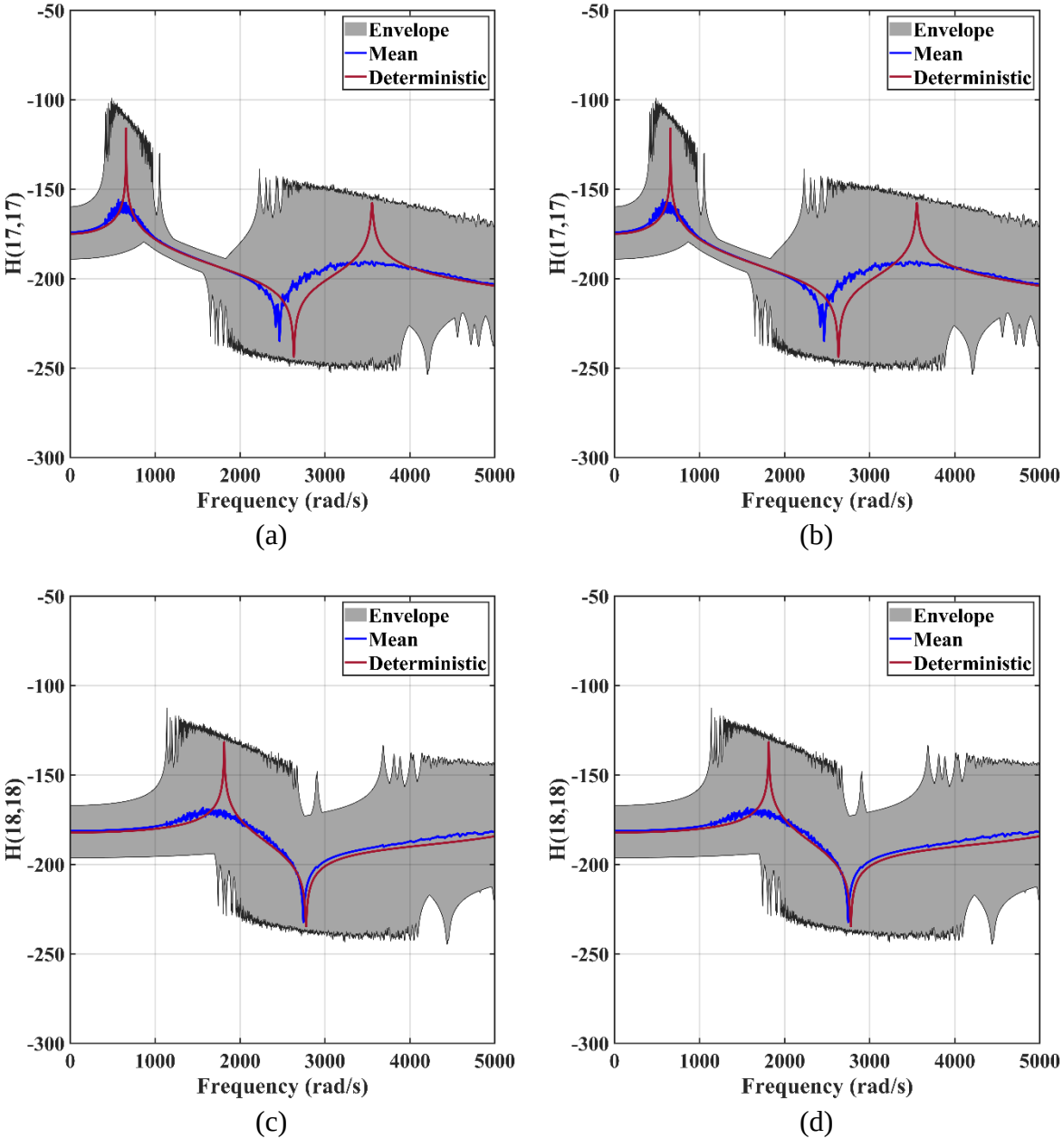

Fig. 7. Displacement FRF band plots (dB) in case I: H(17,17) (a) MCS (b) PM, H(18,18) (c) MCS (d) PM. Note that 10^4 MCS samplesare performed. 35 training points have been employed to construct the PM.

Convergence plots of three different error metrics obtained by estimating the eigen-vectors by using the PM and several other meta-models with increasing numbers of sample points are compared in Fig. 8. The statistical error metrics are given by

$$R^2 = 1 - \frac{\sum_n \left(\boldsymbol{Y} - \widehat{\boldsymbol{Y}}\right)^2}{\sum_n (\boldsymbol{Y} - \bar{Y})^2} \tag{22}$$

$$\text{Root mean square error (RMSE)} = \sqrt{\frac{1}{n}\sum_n \left(\boldsymbol{Y} - \widehat{\boldsymbol{Y}}\right)^2} \tag{23}$$

$$\text{Error } (E) = \sqrt{\sum_n \left(\boldsymbol{Y} - \widehat{\boldsymbol{Y}}\right)^2 \Big/ \sum_n \boldsymbol{Y}^2} \text{ x } 100 \tag{24}$$

where, $\boldsymbol{Y}, \widehat{\boldsymbol{Y}}$ and $\bar{Y}$ denote the true, approximate and mean value of the response quantity, respectively. Note that the error values reported represent the mean obtained by approximating each term of the mode shape matrix.

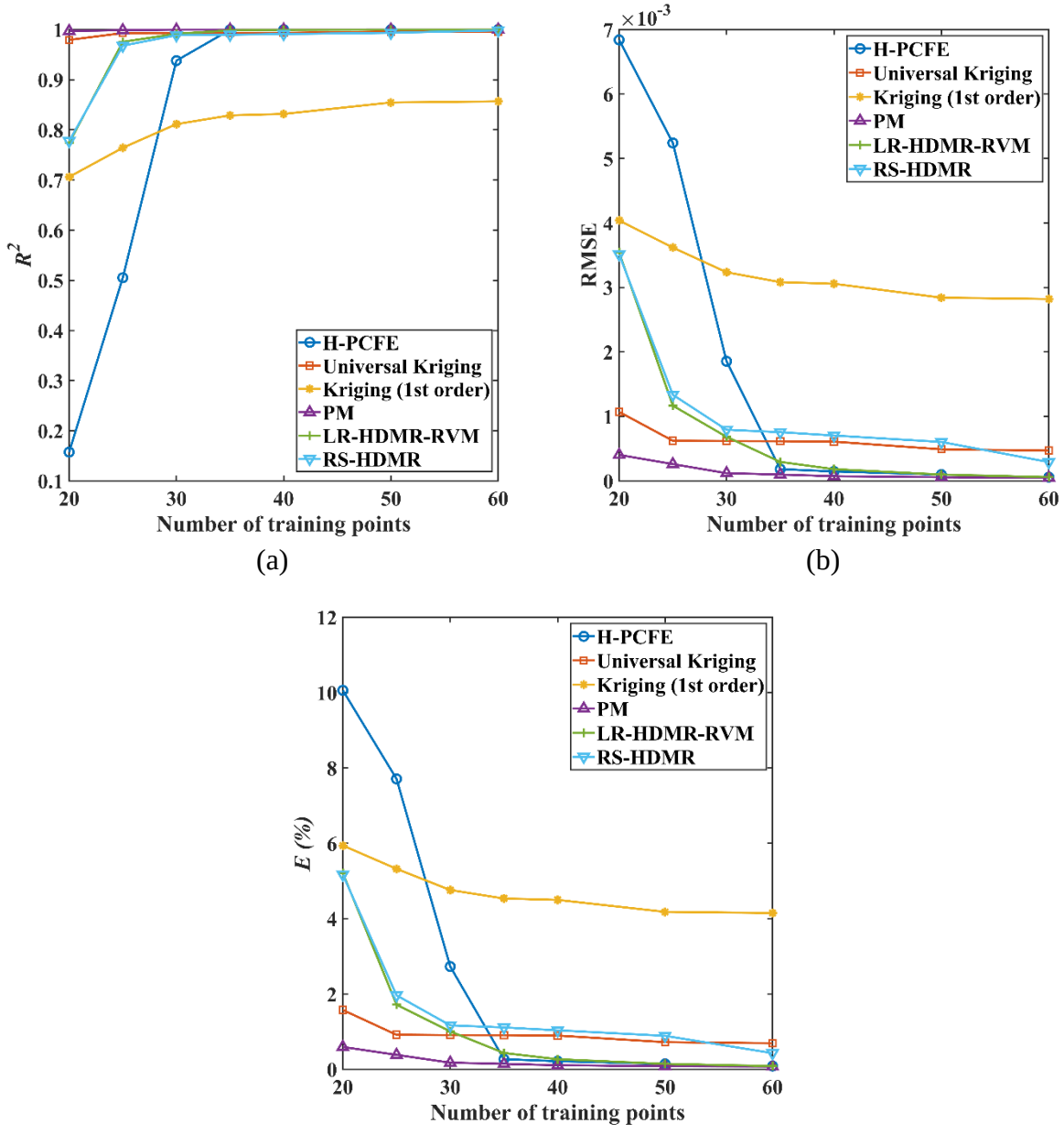

Fig. 8. Convergence of the statistical error metrics (a) R^2 (b) RMSE (c) E (%) with the number of sample points. Note that the error metrics have been evaluated in comparison to 10^4 samples of MCS. H-PCFE denotes hybrid polynomial correlated function expansion (Chatterjee et al. 2016), LR-HDMR-RVM denotes locally refined-high dimensional model representation-relevance vector machine (Chatterjee and Chowdhury 2018b) and RS-HDMR denotes random sampling- high dimensional model representation (Li et al. 2006)

It can be observed from the error values in Fig. 8 that the proposed method (PM) has achieved excellent accuracy. However, the other meta-models have also achieved good results and may easily overtake the PM when solving other example problems. The point worth

highlighting here is that capturing the variational trend of the example problem is straightforward, as expected. The meta-models whose implementation codes are easily available have proven their ability to adequately approximate the eigen-vectors. Thus, the proposed methodology can be easily integrated with already developed in-house stochastic codes by individual research groups.

The results in Fig. 8 correspond to the model approximation errors in the presence of 10% variation in the input parameters. Further, convergence of the mean error metrics obtained using the PM with increasing level of uncertainty are reported in Fig. 9. The results in Fig. 9 demonstrate good approximation accuracy has been achieved by the PM in the presence of high level of input uncertainty which is not often the case with perturbation-based techniques.

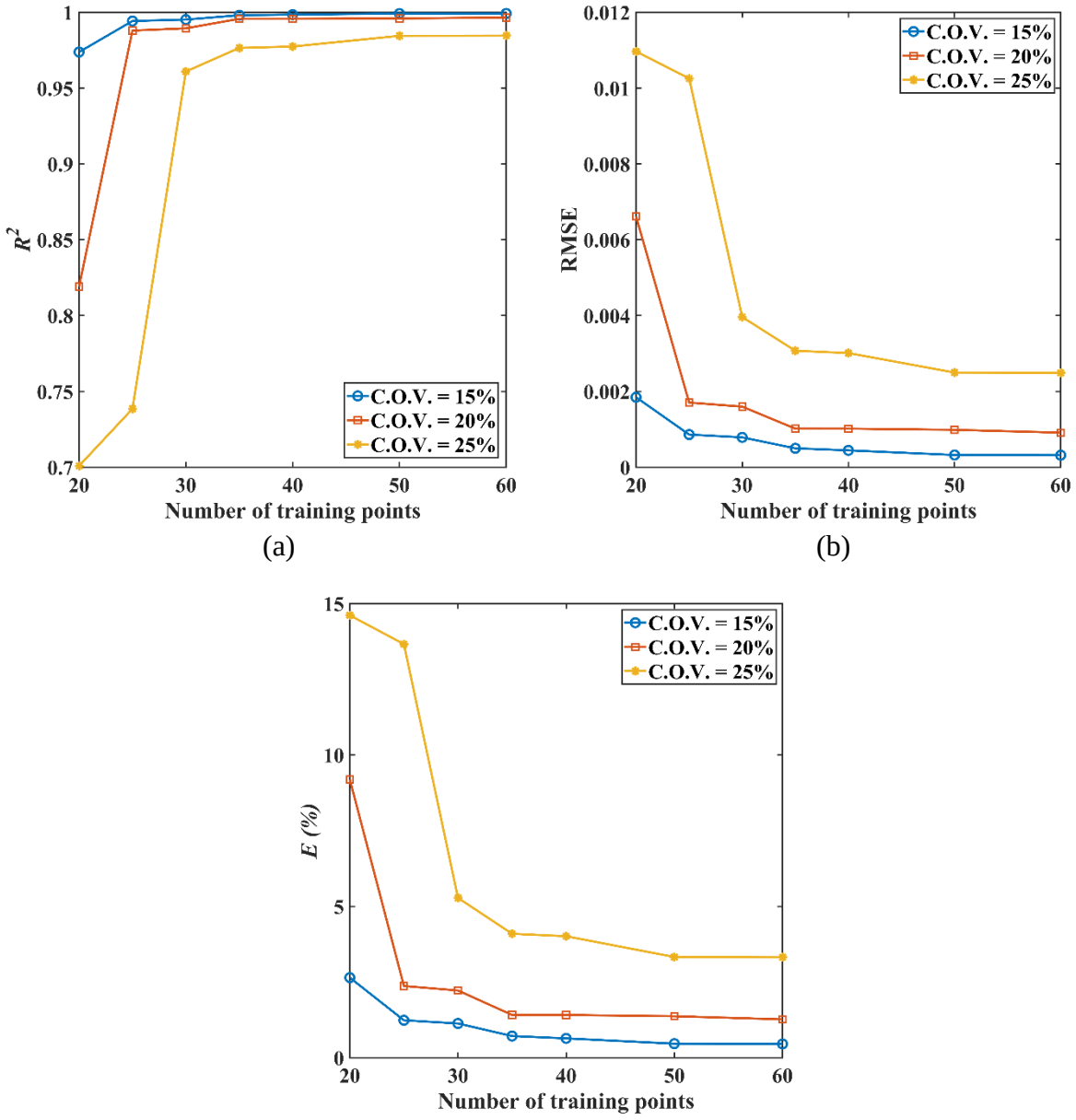

Fig. 9. Convergence of the statistical error metrics (a) R^2 (b) RMSE (c) E (%) obtained by the PM with the number of sample points for increasing levels of input uncertainty. Note that the error metrics have been evaluated in comparison to 10^4 samples of MCS. C.O.V. denotes coefficient of variation.

After illustrating the performance of the proposed methodology in a test example, a large-scale application problem is undertaken in the next section.

6. Practical structural engineering application

A three-dimensional transmission tower model is considered in this section, as presented in Fig. 10. The structure has been modelled as a space frame having six DOFs per node, and thus consists of 175 nodes and 246 elements. The four supports (nodes at level z = 0) are assumed to be fixed in all DOFs. In total, there are 1026 DOFs in the space frame model. The structure was meshed using Gmsh, an open-source meshing software (Geuzaine and Remacle 2009). The mesh details were exported to MATLAB for the finite-element modelling. A snapshot of the mesh with the node locations within the Gmsh environment is presented in Fig. 10.

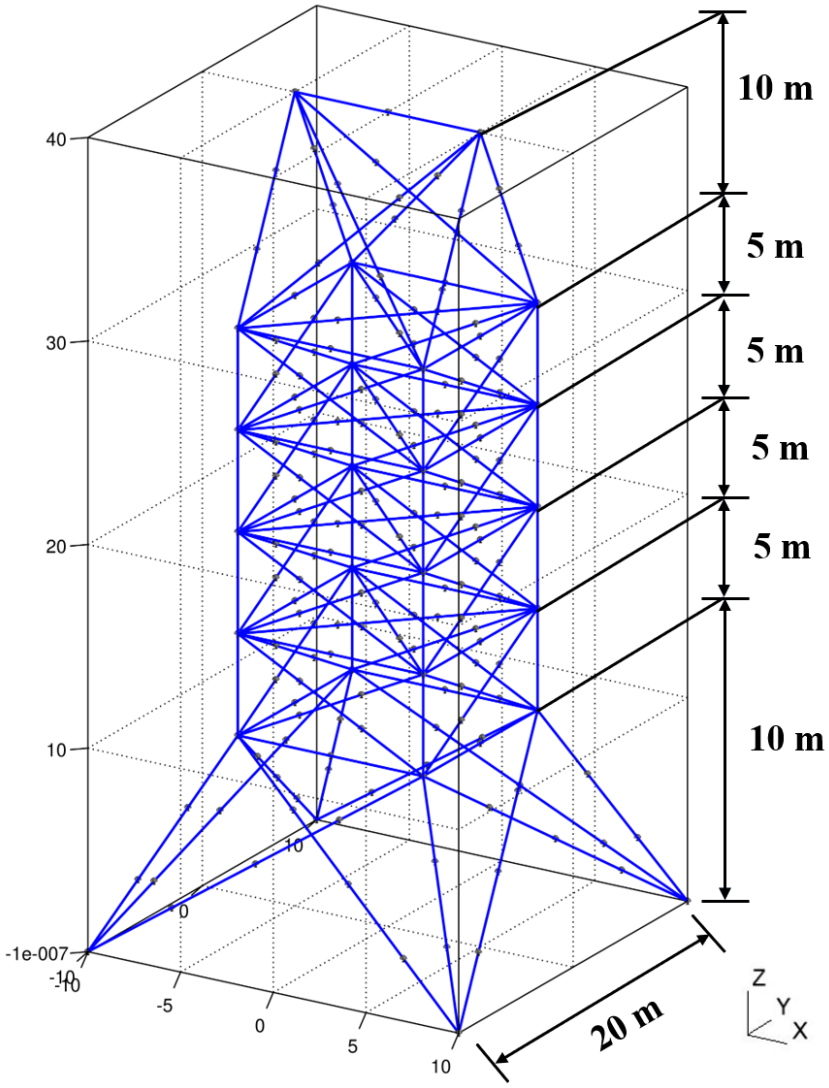

Fig.10. Schematic diagram of the transmission tower model showing the node locations.

Nominal values of material density, namely $\rho = 2700\ \mathrm{kg/m^3}$, elastic modulus $E = 200$ GPa, modulus of rigidity $G = 77$ GPa and a square cross-section with width 0.3 m, are adopted for performing the FE analysis. The damping of the system is assumed to be proportional with the form $\mathbf{C} = \theta\ \mathbf{K}$, where the parameter θ is assumed to be 10^{-3}, and $\mathbf{K}$ is the stiffness matrix.

For implementing the proposed CMS integrated DD framework, the above space frame model has been divided into three sub-components as shown in Fig. 11. The number of internal DOFs corresponding to sub-component 1, 2 and 3 are 114, 600 and 192, respectively. There are two interfaces; the first interface (between sub-component 1 and 2) comprises 72 DOFs and the second interface (between sub-component 2 and 3) comprises 48 DOFs. Note that both interfaces are modelled to include the corner and the remaining nodes at that z-level (Interface 1 at z = 30 m and Interface 2 at z = 10 m). As we are only interested to reduce the internal DOFs of the sub-components, all of the interface DOFs are retained in the subsequent analysis. However, in the presence of a high number of interface DOFs (common in plate structures), they can be easily reduced with the help of characteristic constraint modes.

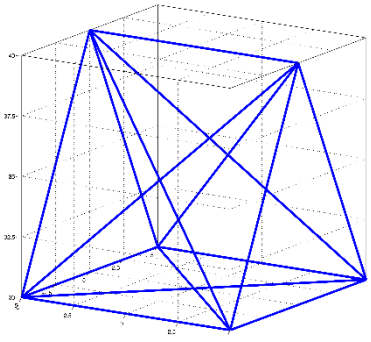

(a)

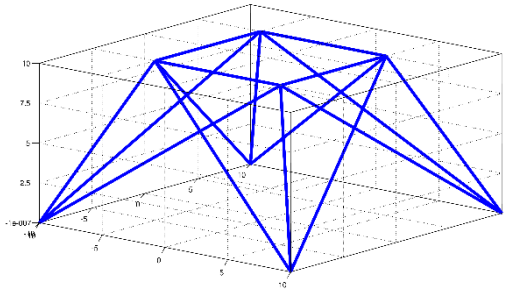

(b)

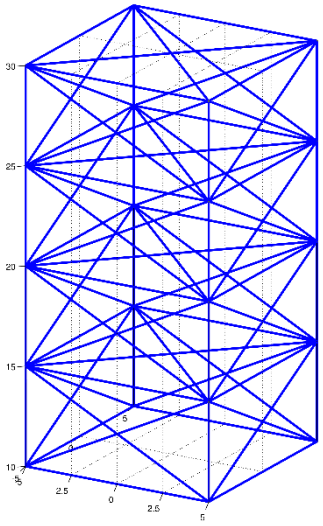

(c)

Fig. 11. Schematic of the sub-components of the space frame model (a) Sub-component 1 (b) Sub-component 3 (c) Sub-component 2.

A similar approach has been adopted to determine the number of modes to be retained in each sub-component, as performed in the previous example (Section 5). The relative L2 error of the Frobenius norm of the frequency response of the deterministic assembled structure has been studied with varying number of modes in the individual sub-components (w.r.t the unreduced model). A reduced model configuration is then selected which is capable of capturing the full model based assembled system response without significant loss of accuracy. The convergence of the error norm with varying number of modes in the sub-components is shown in Fig. 12. Each of the line plots in Fig. 12 corresponds to the error convergence with varying number of modes in one sub-component, when the full models of the other sub-components are considered. Considering the error tolerance value to be 0.04, the number of modes retained from sub-components 1, 2 and 3 are 30, 175 and 78, respectively. This implies that the reduced model utilizes 31% of the internal DOFs compared to the full model in a deterministic sense. Thus, 69% savings in the size of the system matrices can be obtained due to the reduced model configuration w.r.t the full model corresponding to every stochastic simulation. In general, relatively slow convergence has been observed in Fig. 12. This is

primarily due to the definition of the error norm. Since the error norm is based on the whole FRF matrix, insignificant change can be observed in error with varying number of modes. This point is equally relevant for the previous example (Section 5). Alternatively, higher efficiency in terms of model reduction could be achieved by studying the convergence of natural frequencies with specific information of the cut-off frequency or the frequency range of interest.

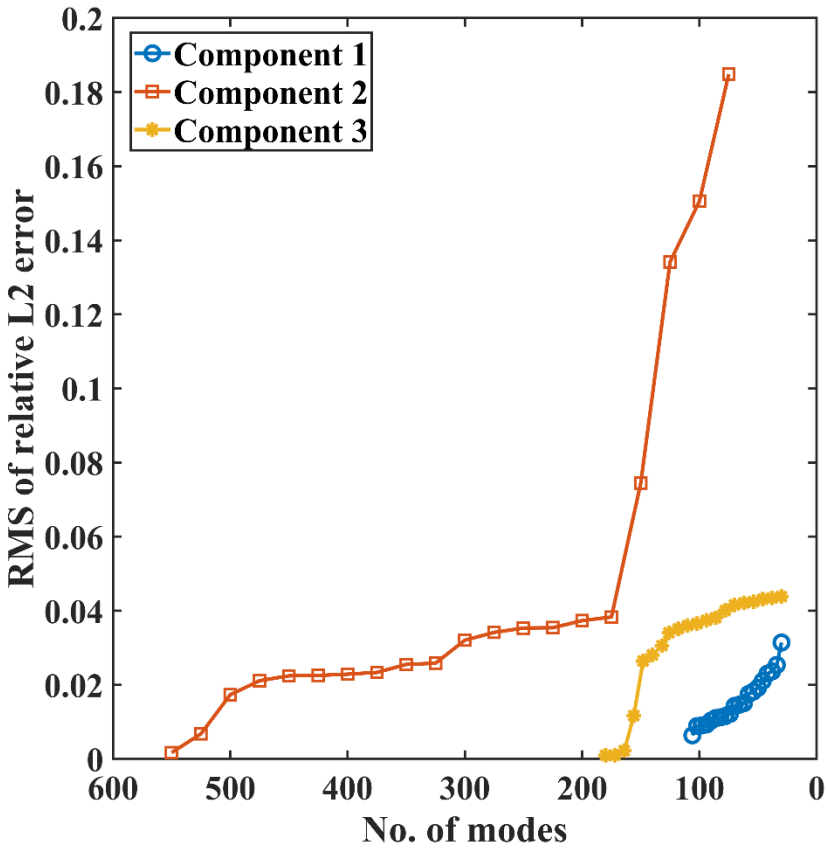

Fig. 12. Convergence of RMS of relative L2 error of the Frobenius norm of the frequency response of the reduced model with respect to the full model with varying number of retained modes in individual sub-components. Note that when the modes of one sub-component are varied, full models of the other sub-components are considered.

To simulate the randomness in the system, the material and geometric properties of each discretized element of the individual sub-systems is considered as stochastic. Specifically, the density, elastic modulus, modulus of rigidity and cross-sectional dimension of each element

is considered to be lognormally distributed with 10% variation. The mean of these parameters is the same as their nominal values reported above.

Gaussian correlation function has been utilized to build the Kriging part of the model. 60 training points have been generated by Latin-hypercube sampling. The PM is trained to approximate the eigen-vectors corresponding to the retained internal DOFs of individual sub-components. Precisely, the dimension of the approximated quantities (mode shape matrix) are (114 x 30), (600 x 175) and (192 x 78) from sub-components 1, 2 and 3, respectively. The stochastic frequency response of the assembled system is obtained by solving the proposed model reduced DD framework as illustrated in Eq. (15) and (16) in conjunction with the PM based prediction of the mode shapes. Sample FRF band plots obtained using MCS (5000 samples) and PM (60 samples) are presented in Fig. 13. Close proximity between the predicted (right side) and actual results (left side) demonstrate that a satisfactory level of approximation accuracy is achieved.

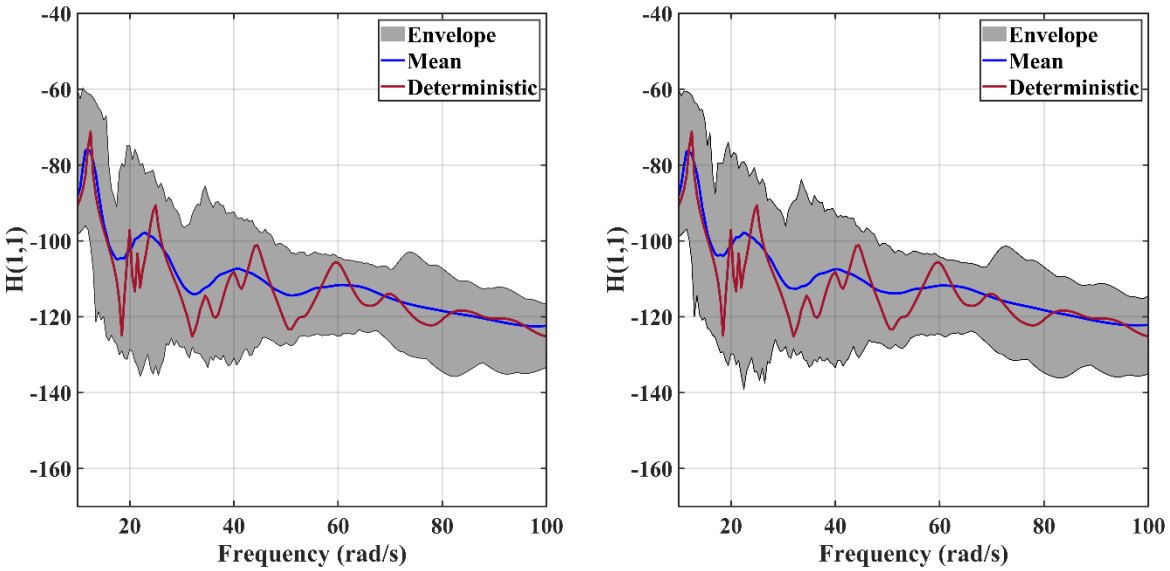

(a) (b)

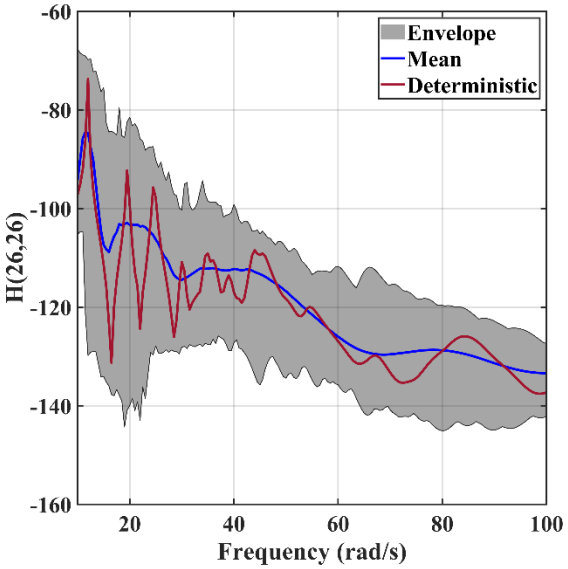
Envelope
Mean
Deterministic
H(26,26)
Frequency (rad/s)

(c)

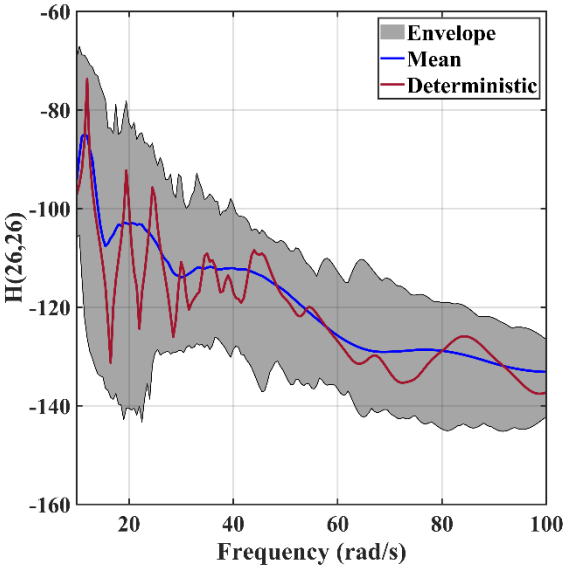
Envelope
Mean
Deterministic
H(26,26)
Frequency (rad/s)

(d)

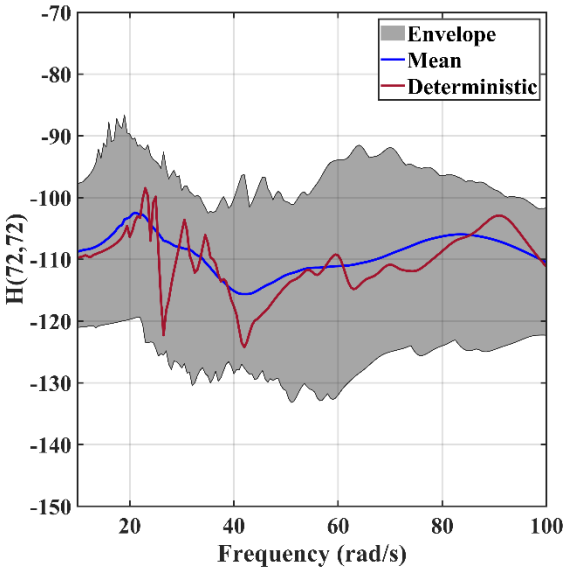
Envelope
Mean
Deterministic
H(72,72)
Frequency (rad/s)

(e)

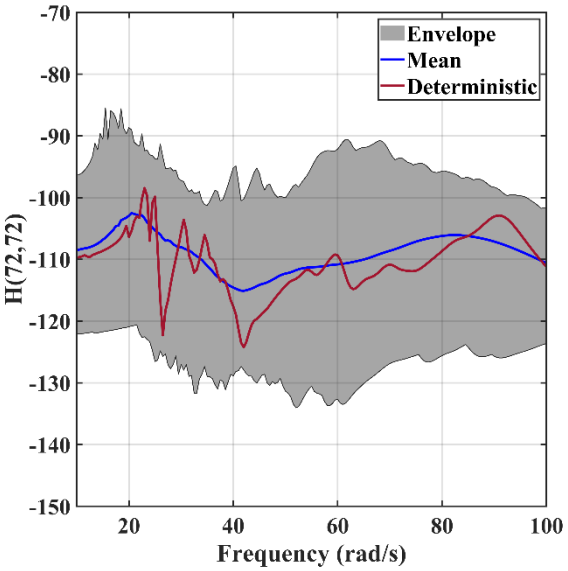
Envelope
Mean
Deterministic
H(72,72)
Frequency (rad/s)

(f)

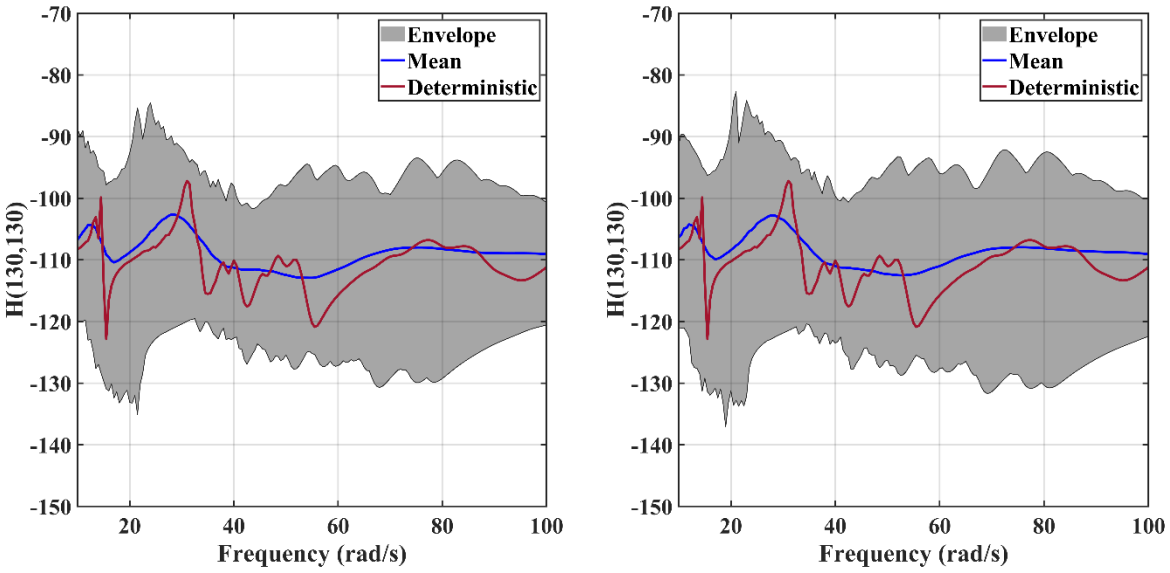

(g) (h)

Fig. 13. FRF band plots (dB): H(1,1) (a) MCS (b) PM, H(26,26) (c) MCS (d) PM, H(72,72) (e) MCS (f) PM, H(130,130) (g) MCS (h) PM. Note that 5000 MCS samples are performed. 60 sample points are used to train PM.

The convergence of the error metrics defined in Eqs. (22)-(24) obtained by approximating the frequency response by the PM with varying numbers of sample points have been presented in Table 1. In doing so, the error metrics are computed with the help of the Frobenius norm of the frequency response obtained by PM and MCS (5000 samples). The errors reported are averaged over the forcing frequency range. The error values obtained in Table 1 illustrate that good approximation accuracy is obtained by the PM. The error values in Table 1 correspond to a 10% variation in the input parameters. Further, the performance of the PM has been assessed for varying levels of input uncertainty in Table 2. In obtaining the results in Table 2, 60 samples were used to train the PM. The error metrics in Table 2 are evaluated in the same way as those of Table 1. The results in Table 2 illustrate reasonable accuracy is obtained by the PM at a 20% uncertainty level with the nominal number of training samples.

Table 1. Convergence of statistical error metrics with varying number of training samples

No. of training points	40	50	60
R^2	0.9517	0.9677	0.9776
RMSE	4.2967×10^{-4}	1.21×10^{-4}	3.6036×10^{-5}
E (%)	7.6225	5.7560	4.8366

Table 2. Convergence of statistical error metrics with varying levels of input uncertainty

C.O.V. (%)	5	10	20
R^2	0.9840	0.9776	0.9340
RMSE	2.3542×10^{-5}	3.6036×10^{-5}	8.4614×10^{-4}
E (%)	4.2204	4.8366	9.5730

7. Summary and conclusions

An efficient framework has been developed for uncertainty propagation from the individual sub-component level to system level response in built-up structures. In doing so, a theoretical framework of dynamic sub-structuring combining model reduction with domain decomposition approach has been presented. The proposed methodology has been initially illustrated in a deterministic configuration of two sub-domains, and then extended for a generalized formulation of multiple sub-domains. Subsequently, the proposed methodology has been explored for application in stochastic dynamic systems. Furthermore, to limit the number of expensive actual simulations, a meta-modelling technique has been presented. The meta-model has the functional form of Kriging with HDMR basis functions and stepwise least squares regression is performed to ensure the orthogonality of the component functions.

A simple stochastic dynamic example has been given to illustrate the performance of the proposed strategy. The approximation capability was demonstrated by the PM, and also some other recently developed and well-known existing meta-models. This illustrates that any other meta-models, whose implementation codes are already available, can be readily used to

approximate the mode shapes and integrated within the proposed methodology. Also, with high levels of input uncertainties, the PM is observed to perform well. Later, a large-scale structural engineering application problem is undertaken where the performance of PM is observed to be satisfactory.

Thus, the main contributions of this work is that the proposed methodology leads to a two-tier improvement in the computational framework of conventional domain decomposition, which are:

- Firstly, the existing computational framework of DD solvers is enhanced by integrating model-order reduction for the local dynamic behaviour of sub-structures together with interface solution problems. This improvement leads to a reduction in the computational effort to solve the actual FE model in a deterministic sense.
- Secondly, in the presence of random parameters at the sub-component level, functional decomposition in the stochastic space efficiently captures the uncertainty propagation from the input variables in individual sub-structures to the assembled system level dynamic response.

Therefore, a bi-level decomposition is performed, one in the physical space and other in the stochastic space. It is worth mentioning that the proposed methodology is generalized so that recent improvements of CMS and DD can be readily integrated.

The method may be extended in terms of further improvements in the computational framework and increasing the complexity of application problems. Re-analysis methods (Perdahcioğlu et al. 2012; Jensen et al. 2016) can be integrated within the proposed approach to further enhance the computational efficiency in stochastic applications, such as optimization under uncertainty. Although this work considers parametric uncertainty modelling, random field modelling can be performed to capture the spatial variability within the sub-components

using the proposed framework. However, for straightforward applicability of the proposed methodology, the spatial randomness would have to be restricted to individual sub-components. Consideration of stochastic correlation across components would require further investigation.

Acknowledgements

The authors gratefully acknowledge the support of the Engineering and Physical Sciences Research Council through the award of a Programme Grant "Digital Twins for Improved Dynamic Design", grant number EP/R006768.

References

Badia S, Martin A, Nguyen H (2019a) Physics-Based Balancing Domain Decomposition by Constraints for Multi-Material Problems. J Sci Comput 79:718–747

Badia S, Martin A, Olm M (2019b) Scalable solvers for complex electromagnetics problems. Finite Elem Anal Des 161:16–31

Bampton M, Craig RRJ (1968) Coupling of substructures for dynamic analyses. AIAA J 6:1313–1319

Bayarri M, Berger J, Cafeo J, et al (2007) Computer model validation with functional output. Ann Stat 35:1874–1906

Bjorstad P, Smith B, Gropp W (1996) Domain Decomposition, Parallel Multilevel Methods for Elliptic Partial Differential Equations. Cambridge University Press: Cambridge, MA

Boo SH, Kim JH, Lee PS (2018) Towards improving the enhanced Craig-Bampton method. Comput Struct 196:63–75

Chatterjee T, Chakraborty S, Chowdhury R (2016) A bi-level approximation tool for the computation of FRFs in stochastic dynamic systems. Mech Syst Signal Process 70–

71:484–505

Chatterjee T, Chakraborty S, Chowdhury R (2019) A Critical Review of Surrogate Assisted Robust Design Optimization. Arch Comput Methods Eng 26:245–274

Chatterjee T, Chowdhury R (2018a) h – p adaptive model based approximation of moment free sensitivity indices. Comput Methods Appl Mech Eng 332:572–599

Chatterjee T, Chowdhury R (2018b) Refined sparse Bayesian learning configuration for stochastic response analysis. Probabilistic Eng Mech 52:15–27

Craig RR (2000) Coupling of substructures for dynamic analyses: an overview. In: Proceedings of AIAA/ASME/ASCE/AHS/ASC Structures, Structural Dynamics, and Materials Conference and Exhibit. pp 1573–1584

Craig RR, Kurdila AJ (2006) Fundamentals of Structural Dynamics. John Wiley & Sons

De Klerk D, Rixen DJ, Voormeeren SN (2008) General framework for dynamic substructuring: History, review, and classification of techniques. AIAA J 46:1169–1181

Desai A, Khalil M, Pettit C, et al (2018) Scalable domain decomposition solvers for stochastic PDEs in high performance computing. Comput Methods Appl Mech Eng 335:194–222

DiazDelaO F, Adhikari S, Saavedra, Flores E, Friswell M (2013) Stochastic structural dynamic analysis using Bayesian emulators. Comput Struct 120:24–32

Dohnal F, Mace BR, Ferguson NS (2009) Joint uncertainty propagation in linear structural dynamics using stochastic reduced basis methods. AIAA J 47:961–969

Dubourg V (2011) Adaptive surrogate models for reliability analysis and reliability-based design optimization. PhD thesis, Universite Blaise Pascal, Clermont-Ferrand, France

Franceschini A, Magri V, Mazzucco G, et al (2019) A robust adaptive algebraic multigrid linear solver for structural mechanics. Comput Methods Appl Mech Eng 352:389–416

Geuzaine C, Remacle J (2009) Gmsh: A 3-d finite element mesh generator with built-in pre- and post-processing facilities. Int J Numer Methods Eng 79:1309–1331

González I V., Valdebenito MA, Correa JI, Jensen HA (2019) Calculation of second order statistics of uncertain linear systems applying reduced order models. Reliab Eng Syst Saf 190:106514

Higdon D, Gattiker J, Williams B, Rightley M (2008) Computer Model Calibration Using High-Dimensional Output. J Am Stat Assoc 103:

Hinke L, Dohnal F, Mace BR, et al (2009) Component mode synthesis as a framework for uncertainty analysis. J Sound Vib 324:161–178

Hung Y, Joseph VR, Melkote S (2015) Analysis of computer experiments with functional response. Technometrics 57:35–44

Hurty WC (1965) Dynamic analysis of structural systems using component modes. AIAA J 3:678–685

Jacquelin E, Adhikari S, Sinou J-J, Friswell M (2015) Polynomial chaos expansion in structural dynamics: accelerating the convergence of the first two statistical moment sequences. J Sound Vib 356:

Jensen HA, Araya VA, Muñoz AD, Valdebenito MA (2017) A physical domain-based substructuring as a framework for dynamic modeling and reanalysis of systems. Comput Methods Appl Mech Eng 326:656–678

Jensen HA, Muñoz A, Papadimitriou C, Vergara C (2016) An enhanced substructure coupling technique for dynamic re-analyses: Application to simulation-based problems. Comput Methods Appl Mech Eng 307:215–234

Kersaudy P, Sudret B, Varsier N, et al (2015) A new surrogate modeling technique combining Kriging and polynomial chaos expansions - Application to uncertainty analysis in computational dosimetry. J Comput Phys 286:103–117

Krattiger D, Wu L, Zacharczuk M, et al (2019) Interface reduction for Hurty/Craig-Bampton substructured models: Review and improvements. Mech Syst Signal Process 114:579–603

Li G, Hu J, Wang SW, et al (2006) Random Sampling-High Dimensional Model Representation (RS-HDMR) and orthogonality of its different order component functions. J Phys Chem A 110:2474–2485

Lu J, Zhan Z, Apley DW, Chen W (2019) Uncertainty propagation of frequency response functions using a multi-output Gaussian Process model. Comput Struct 217:1–17

Mace B, Worden K, Manson G (2005) Uncertainty in structural dynamics. J Sound Vib

288:423–429

Manan A, Cooper J (2010) Prediction of uncertain frequency response function bounds using polynomial chaos expansion. J Sound Vib 329:3348–3358

McKay MD, Beckman RJ, Conover WJ (1979) A comparison of three methods for selecting values of input variables in the analysis of output from a computer code. Technometrics 21:239–245

Mukhopadhyay T, Chakraborty S, Dey S, et al (2016) A Critical Assessment of Kriging Model Variants for High-Fidelity Uncertainty Quantification in Dynamics of composite Shells. Arch Comput Methods Eng. https://doi.org/10.1007/s11831-016-9178-z

Nair PB, Keane AJ (2002) Stochastic Reduced Basis Methods. AIAA J 40:1653–1664

Perdahcioğlu DA, Geijselaers HJM, Ellenbroek MHM, De Boer A (2012) Dynamic substructuring and reanalysis methods in a surrogate-based design optimization environment. Struct Multidiscip Optim 45:129–138

Pichler L, Pradlwarter HJ, Schuëller GI (2009) A mode-based meta-model for the frequency response functions of uncertain structural systems. Comput Struct 87:332–341

Pryse SE, Kundu A, Adhikari S (2018) Projection methods for stochastic dynamic systems: A frequency domain approach. Comput Methods Appl Mech Eng 338:412–439

Rixen DJ (2006) Theoretical Relations Between Domain Decomposition and Dynamic Substructuring. In: Lecture Notes in Computer Science. pp 342–348

Rixen DJ (2004) A dual Craig–Bampton method for dynamic substructuring. J Comput Appl Math 168:383–391

Saad Y (2003) Iterative methods for sparse linear systems. SIAM, Philadelphia, 2nd edition

Sadr M, Astaraki S, Salehi S (2007) Improving the neural network method for finite element model updating using homogenous distribution of design points. Arch Appl Mech 77:795–807

Sarkar A, Benabbou N, Ghanem R (2009) Domain decomposition of stochastic PDEs: Theoretical formulations. Int J Numer Methods Eng 77:689–701

Sarsri D, Azrar L (2016) Dynamic analysis of large structures with uncertain parameters based on coupling component mode synthesis and perturbation method. Ain Shams Eng J 7:371–

381

Sarsri D, Azrar L, Jebbouri A, El Hami A (2011) Component mode synthesis and polynomial chaos expansions for stochastic frequency functions of large linear FE models. Comput Struct 89:346–356

Soize C (2000) A nonparametric model of random uncertainties for reduced matrix models in structural dynamics. Probabilistic Eng Mech 15:277–294

Soize C, Chebli H (2003) Random uncertainties model in dynamic substructuring using a nonparametric probabilistic model. J Eng Mech 129:449–457

Subber W (2012) Domain decomposition methods for uncertainty quantification. PhD Thesis, Department of Civil and Environmental Engineering, Carleton University

Subber W, Sarkar A (2014) A domain decomposition method of stochastic PDEs: An iterative solution techniques using a two-level scalable preconditioner. J Comput Phys 257:298–317

Subber W, Sarkar A (2018) A parallel time integrator for noisy nonlinear oscillatory systems. J Comput Phys 362:190–207

Subber W, Sarkar A (2013) Dual-primal domain decomposition method for uncertainty quantification. Comput Methods Appl Mech Eng 266:112–124

Van den Nieuwenhof, B Coyette J-P (2003) Modal approaches for the stochastic finite element analysis of structures with material and geometric uncertainties. Comput Methods Appl Mech Eng 192:3705–3729

Wan H-P, Mao Z, Todd M, Ren W-X (2014) Analytical uncertainty quantification for modal frequencies with structural parameter uncertainty using a Gaussian process metamodel. Eng Struct 75:

Xia Z, Tang J (2013) Characterization of dynamic response of structures with uncertainty by using Gaussian processes. J Vib Acoust 135:051006

Xiu D, Karniadakis GE (2002) The Wiener--Askey Polynomial Chaos for Stochastic Differential Equations. SIAM J Sci Comput 24:619–644

Yaghoubi V, Marelli S, Sudret B, Abrahamsson T (2017) Sparse polynomial chaos expansions of frequency response functions using stochastic frequency transformation. Probab Eng

Mech 48:39–58

Declaration of interests

☐ The authors declare that they have no known competing financial interests or personal relationships that could have appeared to influence the work reported in this paper.

☒The authors declare the following financial interests/personal relationships which may be considered as potential competing interests:

On behalf of all authors

Tanmoy Chatterjee
23/03/2020